Nearly complete level scheme of ^{116}Sn below 4.3 MeV

S. Raman, T. A. Walkiewicz,* and S. Kahane†
Oak Ridge National Laboratory, Oak Ridge, Tennessee 37831

E. T. Jurney
Los Alamos National Laboratory, Los Alamos, New Mexico 87545

J. Sa,‡ Z. Gácsi,§ and J. L. Weil
University of Kentucky, Lexington, Kentucky, 40506

K. Allaart
Faculty of Physics and Astronomy, Free University, Amsterdam, The Netherlands

G. Bonsignori
Dipartimento di Fisica dell'Universita Bologna, Istituto Nazionale di Fisica Nucleare, Sezione di Bologna, Italy

J. F. Shriner, Jr.
Tennessee Technological University, Cookeville, Tennessee 38505
(Received 15 October 1990)

The level scheme of ^{116}Sn has been studied by combining the results of ^{115}Sn$(n,\gamma)^{116}$Sn and ^{116}Sn$(n,n'\gamma)^{116}$Sn experiments. Both experiments were performed using isotopically enriched samples and Ge γ-ray detectors. Based on the thresholds of γ-ray excitation functions measured for the ^{116}Sn$(n,n'\gamma)$ reaction and the precise γ-ray energies from the capture reaction, 100 levels were observed below 4.3 MeV excitation energy. Approximately half of these were not known previously. Forty-eight of these levels have unique or tentative spin-parity assignments, and for ten more the spin has been restricted to a single value. The spin-parity for most other levels below 4.3 MeV excitation has been restricted to a few values. These spin-parity assignments and limitations were derived mainly from $(n,n'\gamma)$ angular distribution measurements, together with additional information obtained from the cross section magnitudes in both experiments. Above 4.3 MeV excitation energy, 55 additional levels are proposed, based only on the ^{115}Sn(n,γ) results. No J^π information is available for these higher-lying levels beyond the fact that they most probably all have $J \leq 4$. The level scheme below 4.3 MeV from the current work, together with known high-spin levels up to 5.4 MeV seen in other experiments, are compared to the combined predictions of the two-broken-pair model, the interacting boson model, and the deformed collective model. In addition, several states have been phenomenologically identified as proton 1p-1h and collective quadrupole-octupole two-phonon excitations. It is concluded from the good agreement between experiment and these models that all levels in ^{116}Sn with $J \leq 6$ up to an excitation of 4.0 MeV and $J \leq 3$ up to 4.3 MeV may have been experimentally identified. The nearest-neighbor spacing distribution is intermediate between that of a Gaussian orthogonal ensemble and that of a Poisson distribution, with a slight preference for the former. The neutron separation energy was determined to be 9563.47±0.11 keV.

I. INTRODUCTION

Low-lying nuclear energy levels (say, below ~2.5 MeV excitation energy) have been studied for several decades and have provided guidance for the development and refinement of nuclear models. Occasionally these levels (or, more correctly, the density of these levels) have served as anchors for those expressions of nuclear level densities that deal primarily with the compound resonances. Only recently have the statistical properties (level densities, spacing distributions, etc.) of these bound levels become the subject of detailed investigations.[1–3] This delay is at least in part due to the requirement that, for meaningful statistical interpretation, the level scheme for a particular nucleus needs to be as "complete" as possible; that is, all levels of either parity should be known within a specified spin window. Furthermore, the excitation energy range should be wide enough to encompass a large number of levels. If this number is required to be, say ≥80, the number of nuclei with "complete" level schemes is quite small. To advance the study of the statistical properties of low-lying levels, it is therefore highly desirable to acquire data on many more nuclei throughout the periodic table. The study of ~100 levels (below 4.3 MeV) in ^{116}Sn constitutes the main topic of this paper. This study utilized the ^{115}Sn(n,γ) and the

^{116}Sn$(n,n'\gamma)$ reactions.

Radioactive decay studies[4–9] and nuclear reaction studies[10–35] have contributed information on approximately 55 states in ^{116}Sn below 4.3 MeV. These measurements have been explicitly identified in Table I, and the data have been summarized in the Nuclear Data sheets.[36]

The (n,γ) reaction is well known to provide a sensitive method for studying a large number of states, regardless of their structure, within a narrow spin-parity range. Inelastic neutron scattering offers another favorable reaction for studying low-lying excitations because the neutron energies can be varied very close to threshold for a particular excitation, thus eliminating unwanted effects from the population of higher-lying levels and allowing the threshold for exciting the state to be observed. Because of the excellent energy resolution of γ-ray detectors, close-lying levels can be more easily resolved with the $(n,n'\gamma)$ reaction than with charged particle scattering or reactions. Level excitation by (n,n') is limited only by the total angular momentum that the scattered particle brings into the system. On the other hand, the sensitivity of $(n,n'\gamma)$ enables the measurement of cross sections spanning three orders of magnitude. Coupling these capabilities of the $(n,n'\gamma)$ reaction with the sensitivity, the high precision of γ-ray energy determination, and nonselectivity of level excitation in the (n,γ) reaction provides a powerful tool for developing a complete level scheme at low excitation energies.

The ^{115}Sn nucleus has an appreciable thermal neutron-capture cross section ($\approx$40 b) but low natural abundance

TABLE I. Partial list of references to previous measurements on ^{116}Sn levels. See the Nuclear Data Sheets (Ref. 36) for a more complete list.

Measurement	Author(s)	Reference
14-sec ^{116}In β^- decay	Okano and Kawase	4
54-min ^{116}In β^- decay	Rabenstein	5
	Ardisson	6
	Yamaguchi *et al.*	7
16-min ^{116}Sb $(\beta^+ + \varepsilon)$ decay	Gehrke and McIsaac	8
	Riedinger *et al.*	9
60-min ^{116}Sb $(\beta^+ + \varepsilon)$ decay	Gehrke and McIsaac	8
^{114}Cd$(\alpha,2n\gamma)$ reaction	Yamazaki and Ewan	10
	van Poelgeest	11
	Bron *et al.*	12
	van Poelgeest *et al.*	13
^{115}In$(\alpha,t\gamma)$ reaction	Schippers	14
^{115}In$(^3$He,$d)$ reaction	Biggerstaff *et al.*	15
	Shoup *et al.*	16
	van der Werf *et al.*	17
^{115}Sn(n,γ) reaction	McClure and Lewis	18
	Rudak *et al.*	19
^{115}Sn(d,p) reaction	Schneid *et al.*	20
^{116}Cd$(^3$He,$n)$ reaction	Fielding *et al.*	21
^{116}Sn(e,e') reaction	Phan Xuan Ho *et al.*	22
	van der Werf *et al.*	17
^{116}Sn(p,p') reaction	Allan *et al.*	23
	Beer *et al.*	24
	Wienke *et al.*	25
^{116}Sn$(\vec{p},p')$ reaction	van der Werf *et al.*	17
^{116}Sn$(p,p'\gamma)$ reaction[a]	Bäcklin *et al.*	26
	Kantele *et al.*	27
	Bäcklin *et al.*	28
	Jonsson *et al.*	29
^{116}Sn$(n,n'\gamma)$ reaction	Demidov *et al.*	30
^{116}Sn(d,d') reaction	Kim and Cohen	31
^{116}Sn$(^{16}$O,^{16}O$'\gamma)$ reaction	Kantele *et al.*	27
	Bäcklin *et al.*	28
	Jonsson *et al.*	29
^{117}Sn(p,d) reaction	Yagi *et al.*	32
	Fleming	33
^{117}Sn(d,t) reaction	Schneid *et al.*	20
	Schreuder *et al.*	34
^{117}Sn$(^3$He,$\alpha)$ reaction	Schreuder *et al.*	34
^{118}Sn(p,t) reaction	Yagi *et al.*	32
	Fleming *et al.*	35

[a]Including conversion electron measurements.

(0.35%). Two studies of the ^{115}Sn(n,γ) reaction have been reported previously. McClure and Lewis[18] utilized an external neutron beam facility and a target consisting of 2.8 g of Sn enriched to 30% in ^{115}Sn. They observed six definite and three possible primary transitions and $\sim$60 secondary transitions. Their level scheme consisted of 21 excited states in ^{116}Sn. The overall agreement is good between the data of McClure and Lewis[18] and the more extensive data of the current study. Rudak *et al.*[19] have presented a table of energies and intensities of 71 transitions from the ^{115}Sn(n,γ) reaction but give no other details. Their relative intensities are in reasonable agreement with the current values for γ-ray energies below 2.2 MeV, but their intensity values for higher-energy γ rays differ from ours by a factor of $\sim$3.

Demidov *et al.*[30] have studied the $(n,n'\gamma)$ reaction with fast neutrons from a reactor using an 8-g Sn target enriched to 96.8% in ^{116}Sn. Below 3.5 MeV, these authors observed $\sim$65 γ rays that were incorporated into a level scheme consisting of $\sim$30 states below 3.9 MeV. The results of Demidov *et al.*[30] are, in general, consistent with the current, more extensive study.

The organization of this paper is as follows. The (n,γ) and $(n,n'\gamma)$ measurements are described in Sec. II. The construction of a decay scheme as extensive as the current one is a long and complicated process and is outlined in Sec. III. Whether all existing levels up to a certain energy have indeed been observed is a question that is difficult to answer. An indication of failure could be a larger number of levels predicted by generally accepted and well-established models than are found experimentally. The results of model calculations are discussed at some length in Sec. IV. Good overall agreement between the number of observed and calculated levels is established in Sec. V. The fluctuation properties of a subset of levels are tested in Sec. VI to search for possible chaotic behavior. Finally, a summary is provided in Sec. VII.

II. EXPERIMENTAL PROCEDURE AND ANALYSIS

A. ^{115}Sn(n,γ) measurements

The (n,γ) measurements were made at the internal target facility of the Los Alamos Omega West Reactor. A detailed description of this facility has been presented in an earlier paper on the sulfur isotopes.[37] The target position was 1.5 m from the edge of the reactor core. The thermal-neutron flux at this position was nominally 6×10^{11} neutrons/(cm^2 sec). The γ rays were studied with a 26-cm^3 coaxial Ge(Li) detector positioned inside a NaI(Tl) annulus. This detector was located 6.3 m from the target and was operated in either a Compton-suppressed or pair-spectrometer mode. The system resolution (full width at half maximum) was typically 2.3 keV at 1 MeV, 5.5 keV at 6 MeV, and 8.8 keV at 11 MeV. Typical spectra are shown in Figs. 1 and 2.

These (n,γ) measurements utilized a 13.0-mg target enriched to 97.3% in ^{115}Sn. This target was prepared[38] by a "second pass" of a small amount of ^{115}Sn that had been enriched earlier to $\approx$30%. This starting material was originally part of the Research Materials Collection maintained by the Oak Ridge National Laboratory. Over 400 γ rays in the 0.1- to 9.6-MeV region were identified in this experiment. Gamma rays above 1 MeV with intensities as low as 5 photons per 10^4 captures were detected; below this energy, the sensitivity was even better by a factor of about 3.

The procedures employed to establish the energy and intensity calibrations have been described in earlier papers.[37,39,40] Briefly, the γ-ray energies are based mainly on the "gold standard" (see Ref. 40) below 2.2 MeV and on the "mass-doublet standard" above. The latter is derived from the neutron binding energies of ^{2}H, ^{13}C, and ^{15}N (see Table I of Ref. 40). Subsequent revisions and adjustments strongly suggest[40] that the vast bulk of the $>$2-MeV γ rays reported in this paper should be lowered by an amount not exceeding 100 eV. Because the construction of the level scheme depends more on energy differences than on absolute energy values, we have made no attempt to apply this correction except when reporting the final neutron separation energy.

The energy dependence of the detector efficiency in the Compton-suppressed mode was determined from a set of radioactive sources (^{24}Na, ^{56}Mn, ^{82}Br, ^{152m}Eu, etc.) with calibrated γ-ray intensities.[41] The efficiency curve in the double-escape mode was derived from the relative intensities of the γ rays from the ^{14}N(n,γ) reaction (see Table IV of Ref. 39). The capture cross sections reported in this paper are based on $\sigma_\gamma(2200\ \text{m/s})=332\pm2$ mb for ^{1}H (Ref. 42).

The spin and parity of the ^{115}Sn ground state are $\frac{1}{2}^+$. Thermal-neutron (s-wave) capture, therefore, leads to a 0^+ or 1^+ capturing state. Based on prior experience, all low-spin states ($J\leq3$) should be readily observable (via primary and/or secondary transitions) in the (n,γ) measurement up to $\sim$40% neutron separation energy (4 MeV in this case). Conversely, if it can be definitely established that a particular level is populated weakly, or not at all, its spin is most probably ≥4.

B. ^{116}Sn$(n,n'\gamma)$ measurements

The $(n,n'\gamma)$ measurements were made at the 6.5-MV Van de Graaff Laboratory of the University of Kentucky. A pulsed proton beam of 2 μA with 2-MHz repetition rate passed through a 3.5-μm-thick Mo window into a 3-cm-long gas cell containing 1 atm of tritium. Monoenergetic neutrons from the ^{3}H$(p,n)^3$He reaction, with an energy spread of 50 to 80 keV depending on the proton energy, were incident on a cylindrical scattering sample located at 0° with respect to the incident proton beam and 5.5 to 6.5 cm from the end of the gas cell. The scattering sample (also part of the Research Materials Collection maintained by the Oak Ridge National Laboratory) had a mass of 42.6 g and was enriched to 95.7% in ^{116}Sn. Further details on sample impurities and dimensions are given in Ref. 43. The emitted γ rays were detected with a high-purity Ge detector with 21% efficiency, except for the excitation function measurements from 1.9 to 3.4 MeV, for which a 25% efficient Ge(Li) detector was used. Both detectors had an energy resolution of ≤2 keV at 1.33 MeV. They were shielded from room-scattered neu-

trons by a lead annulus inside a 60-cm cube of borated polyethylene behind a massive (50-cm-thick) copper collimator, and shielded from the direct neutron flux by a 50-cm-long tungsten shadow bar. The sample-to-detector distance was 1 m.

Time-of-flight (TOF) methods were used to obtain suppression, relative to the prompt γ rays, of scattered neutron signals and of time-uncorrelated background. Germanium detectors are well known to have a large rise-time variation in their output signals along with some correlation of very slow rise times with the small signals for low-energy events in the detector. To decrease the time spread of the γ-ray signals and also increase the dynamic range of the detection system, a rise-time compensation method was used.[44,45] Gamma rays from 90 to 4300 keV were detected with good efficiency using this method. Because no γ rays assigned to ^{116}Sn were observed below 350 keV, a simpler fast-trigger scheme was used for the angular-distribution measurements. A typical γ-ray spectrum, measured at an incident neutron energy of 4.5 MeV to show the whole range of detected γ rays, is given in Fig. 3. Approximately 180 γ rays were identified in the $(n,n'\gamma)$ measurements.

Three types of γ-ray measurements were made. The

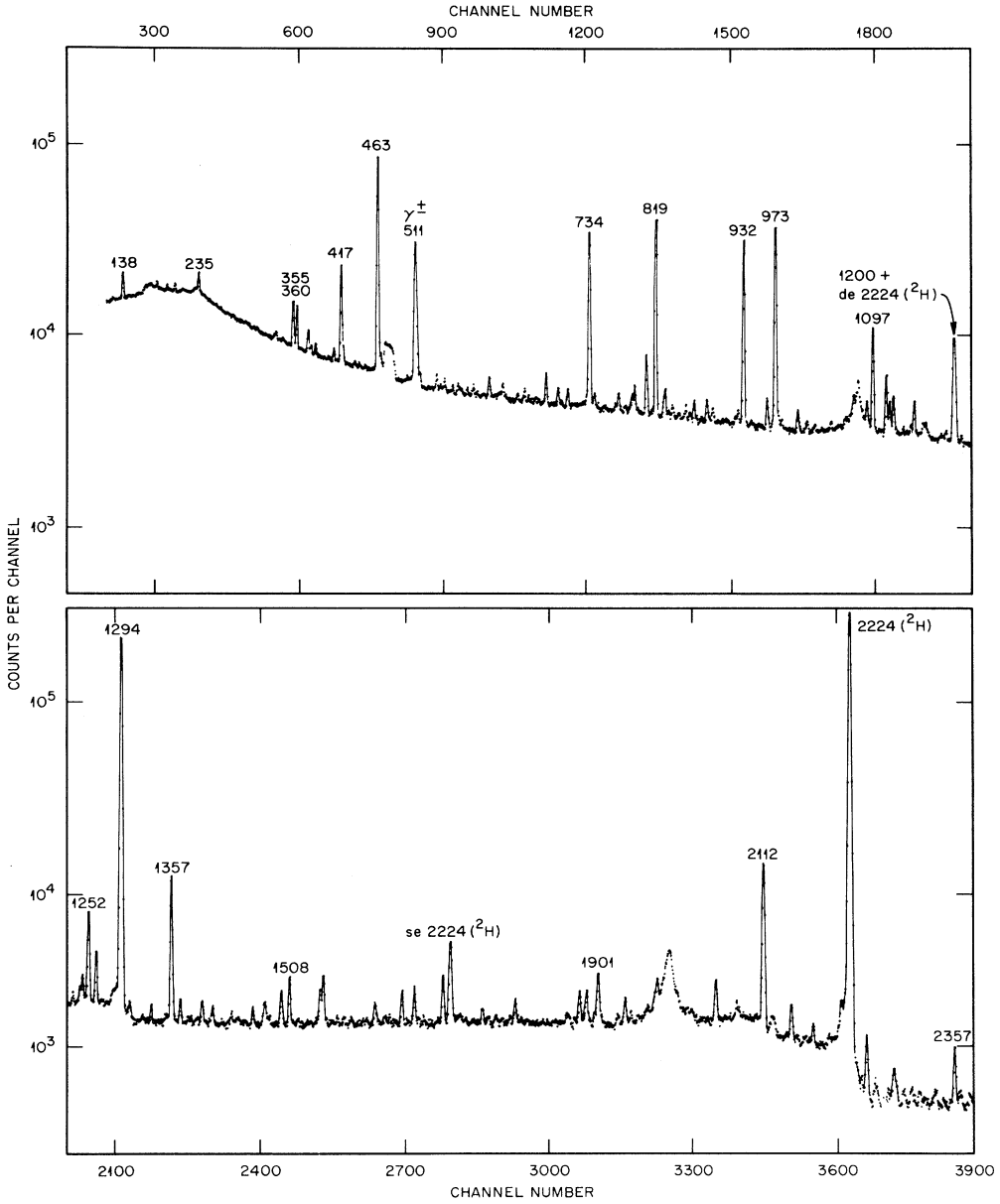

FIG. 1. Gamma-ray spectra from thermal neutron capture by ^{115}Sn. The Ge(Li) detector was operated in the Compton-suppression mode. All energies are in keV. A detailed list of γ rays observed in ^{116}Sn is given in Table II.

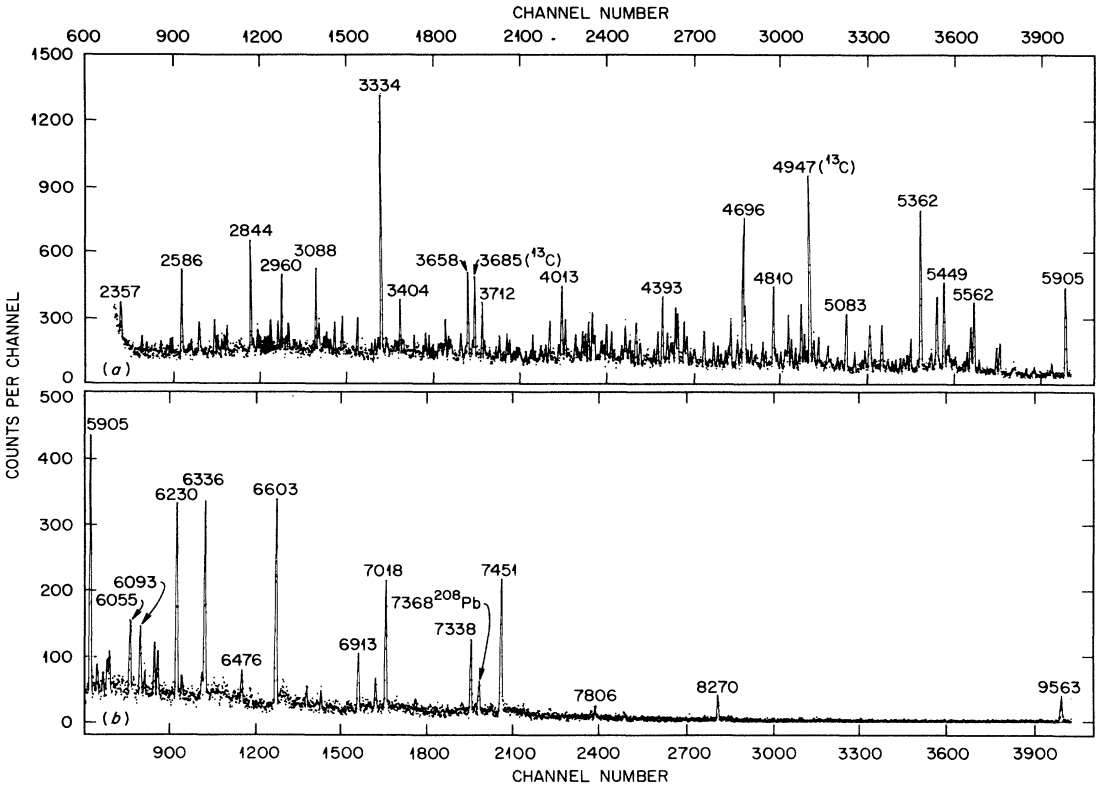

FIG. 2. Gamma-ray spectra from thermal neutron capture by ^{115}Sn. The Ge(Li) detector was operated in the pair-spectrometer mode. All energies are in keV. A detailed list of γ rays observed in ^{116}Sn is given in Table II.

excitation functions of the prompt γ rays were measured at 90° to the incident neutron direction over the neutron energy range of 1.9 to 4.5 MeV, mostly in steps of 50 keV. This measurement determines thresholds for excitation of the various excited states and is one of the main pieces of information used in this work for placing a γ ray in the decay scheme. Angular distributions of the prompt γ rays were measured to determine, or at least limit, the spin and sometimes the parity of the emitting state. In several cases the angular-distribution analysis made possible a unique placement of a particular γ ray in the decay scheme because no J^{π} choice for the other energetically allowed placements was consistent with the experimental data. By placing a gate on signals in the

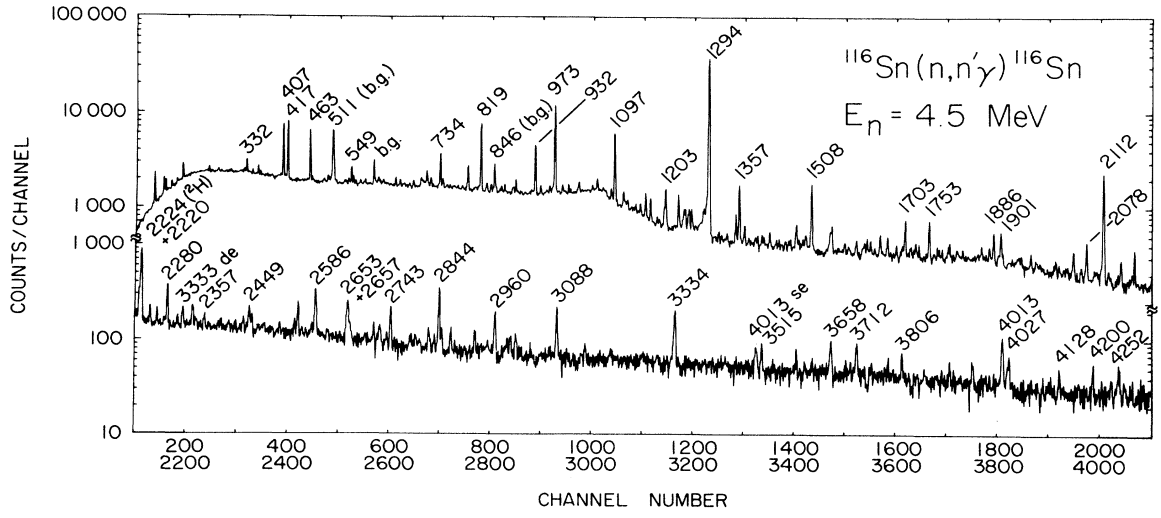

FIG. 3. Gamma-ray spectra from the ^{116}Sn$(n,n'\gamma)$ reaction at an incident neutron energy of 4.5 MeV. All energies are in keV. A detailed list of γ rays observed in ^{116}Sn is given in Table II.

TOF spectrum occurring at times after the prompt γ peak, delayed γ rays emitted by levels of ^{116}Sn with lifetimes in the nanosecond-to-microsecond range were detected. Doppler shift attenuation (DSA) methods were applied to angular distribution results to determine lifetimes in the range of 10–400 fs. The details and results of the angular distribution and lifetime measurements will be presented in a future paper.

In the excitation function measurements, the incident neutron flux was monitored with a long counter possessing an approximately energy-independent response. For the angular distribution measurements, an NE218 liquid scintillator with pulse-shape discrimination was operated in the TOF mode as a fixed-angle neutron monitor.

The γ-ray yields were corrected for relative detector efficiency and sample-size effects; the latter included neutron absorption and multiple scattering, γ-ray absorption, and γ-ray yield enhancement due to secondary-neutron inelastic scattering (for $E_\gamma = 1293$ keV only). Details of these corrections are given in Ref. 46. The relative efficiency of the γ-ray detectors was measured using radioactive sources of ^{56}Co, ^{133}Ba, ^{152}Eu, and ^{228}Th that emit γ rays between 50 and 3600 keV with accurately known relative intensities.[41] Because the γ-ray energies were much more precisely determined in the (n,γ) experiment, the energy calibration for the $(n,n'\gamma)$ spectra was taken from those γ rays that were strong in both experiments.

The absolute cross sections for γ-ray production were determined by normalizing to the yield of the 847-keV γ ray from ^{56}Fe$(n,n'\gamma)$, which was measured concurrently at 400–500-keV intervals. The angular distributions were normalized in the same manner. The ^{56}Fe production cross sections $\sigma_{847}(E_n, 90°)$ were taken from an updated compilation,[47] an earlier version of which has been published.[48] The details of the normalization procedure and of the determination of cross section uncertainties are given in Ref. 46, as well as a more extensive discussion of the rest of the experimental procedures.

The initial analyses of the (n,γ) and $(n,n'\gamma)$ measurements were made without the benefit of mutual interaction, and the preliminary results were reported separately.[49,50] Exchange of data ensued, and it soon became apparent that the two data sets were highly complementary. The results obtained by combining them were also reported previously in a preliminary form.[51] The final results are reported in this paper and in one other to follow.

III. DECAY SCHEME FOR ^{116}Sn

The experimental results from this work are presented in Tables II–V. In Table II are listed all γ rays, together with their proposed level placements, seen in the ^{116}Sn$(n,n'\gamma)$ and ^{115}Sn(n,γ) experiments. The absolute intensities in barns are given for γ rays seen in (n,γ), and for the decays seen in $(n,n'\gamma)$, the threshold energies derived from the excitation functions are tabulated. Table III gives the level scheme (energies only) resulting from the current work. The γ-branching ratios of those levels that are either not fed, or fed only weakly, in the (n,γ) reaction can be found in Table IV. Table V gives the level scheme from both experiments up to 4300 keV excitation energy, spin and parity assignments, and γ-ray intensity balance for those levels populated in the (n,γ) reaction. Table V also summarizes previous results on the ^{116}Sn level scheme.

A. Levels below 4.3 MeV

An initial level scheme was constructed on the basis of threshold energies and γ-ray energies measured in the $(n,n'\gamma)$ experiment. For those γ rays seen in both the (n,γ) and $(n,n'\gamma)$ experiments (see Table II), the more precise γ-ray energies from the (n,γ) work were employed. Because the excitation functions were not measured below $E_n = 1.9$ MeV, no thresholds were observed for the well-known first- and second-excited states at $E_x = 1293$ and 1757 keV, respectively, but for all other levels up to an excitation energy of 4297 keV (with the exception of the known levels at 2909.6, 3277.3, and 3706.9 keV), there was a measured threshold that established the position of the level. In a few cases, which are discussed below, there is an ambiguity of up to 150 keV in the placement of a γ ray and the associated level energy. Details of some unusual excitation functions are also discussed below.

Having established the basic framework of levels up to $E_x = 4297$ keV, the Ritz combination principle was employed to place additional γ rays seen in (n,γ), but not in $(n,n'\gamma)$, into this part of the decay scheme. The good precision of the (n,γ) γ-ray energies was very useful in determining such placements. During this process approximately 50 of these transitions were correlated with very weak γ rays in the $(n,n'\gamma)$ spectra, and their excitation functions were checked to ensure their correct placement in the decay scheme. For each γ ray seen only in the (n,γ) experiment, it was verified that the branching ratio was such that the transition would be below the limit of sensitivity of the $(n,n'\gamma)$ experiment.

The requirement that all γ-ray placements be consistent with the $(n,n'\gamma)$ threshold energies, the maintenance of a reasonable intensity balance at each level, the good precision of the E_γ values from (n,γ), and the agreement of the branching ratios in both experiments have combined to produce a level scheme up to $E_x = 4297$ keV which has very few ambiguous placements. Possible ambiguities are discussed in Sec. III C. The requirement that each placement satisfy so much measured information has also led to the inference that there are several cases where two γ rays with quite similar energies deexcite different levels. Some of these cases are also discussed below.

B. Excitation functions

Typical $(n,n'\gamma)$ excitation functions of γ decays from levels which are populated directly by neutron scattering, and not significantly by γ decays from higher-excited states, are shown in Fig. 4(a). These energy-dependent cross sections can be calculated quite well from the statistical model[52–55] for compound-nucleus formation and decay,

TABLE II. Energies (E_γ), photon intensities (I_γ), threshold energies (E_{th}), and placements of γ rays in ^{116}Sn from the ^{115}Sn(n,γ) and the ^{116}Sn$(n,n'\gamma)$ reactions.

(n,γ) E_γ (keV)[a]	(n,γ) I_γ (b)	$(n,n'\gamma)$ E_γ (keV)[b]	$(n,n'\gamma)$ E_{th} (keV)[c]	Placement
99.9[d] *5*	0.11 *3*			2366.1
125.66 *30*	0.003 *1*			3469.7
138.39 *4*	0.041 *4*			2529.2
181.96 *7*	0.013 *2*			?
194.83 *9*	0.012 *2*			2996.3
204.96 *6*	0.019 *2*			2790.6
235.24 *6*	0.052 *6*			?
305.65 *26*	0.006 *2*			?
309.75 *22*	0.010 *3*			2960.1
331.80 *18*	0.011 *2*	331.7 *4*	3150 *30*	3105.4
333.94 *10*	0.019 *3*			?
338.4 *4*	0.005 *1*			?
342.0 *3*	0.009 *3*			?
343.9 *4*	0.006 *2*	344.0 *5*	3340 *50*	?
		355.0 *9*	3400 *150*	3350.6
355.492 *24*	0.16 *3*	355.4 *4*	2160 *40*	2112.3
360.173 *25*	0.14 *2*	360.4 *4*	2650 *50*	2585.6
374.52 *6*	0.067 *8*	374.6 *5*	2900 *100*	2960.1
378.24 *14*	0.022 *3*	378.5 *5*	3150 *150*	3179.7
384.22 *6*	0.032 *5*	384.3 *5*	2650 *100*	2650.5
407.43 *11*	0.027 *5*	407.5 *3*	2800 *30*	2773.6
		407.5 *3*	3400 *100*	3453.9
416.86[e] *3*	0.39[e] *6*	417.0 *3*	2540 *20*	2529.2
417.4[e] *4*	0.08[e] *3*	417.4 *4*	4200 *200*	4076.0
419.60 *12*	0.044 *7*			3508.4
433.90 *26*	0.019 *6*			2545.7
		436.5 *6*	< 4500	3210.1
439.32 *17*	0.013 *4*			3952.9
463.249 *26*	2.8 *4*	463.4 *2*	1750 *100*	1756.8
466.7 *6*	0.052 *19*	466.8 *6*	3050 *50*	2996.3
500.84 *20*	0.013 *2*			3344.4
		503.3 *6*	3200 *300*	3032.2
		535.5 *6*	3400 *200*	3309.2
538.21 *6*	0.045 *7*	538.2 *7*	2650 *150*	2650.5
		543.5 *5*	< 3200	2909.6
548.34 *9*	0.036 *5*			3508.4
		549.1 *4*	3370 *30*	3350.6
558.47 *12*	0.015 *3*			?
565.16 *12*	0.025 *4*			2790.6
		568.0 *6*	3050 *60*	3097.3
577.36 *25*	0.011 *5*			2843.8
584.98 *16*	0.040 *7*			?
605.34 *6*	0.069 *9*	605.3 *6*	3100 *100*	2996.3
		615.6 *6*	< 3900	?
622.68 *9*	0.041 *6*			?
		641.1 *4*	3150 *150*	3032.2
641.63 *14*	0.027 *4*			3227.5
650.46 *8*	0.047 *6*	650.3 *4*	3200 *150*	3016.6
655.60 *16*	0.020 *4*	656.2 *6*	< 3750	3046.4
664.54 *20*	0.016 *3*			3508.4
668.5 *4*	0.011 *2*			3469.7
675.6 *5*	0.009 *3*			?
678.28 *5*	0.122 *14*	678.2 *5*	2800 *70*	2790.6
693.82 *6*	0.078 *9*			2960.1
698.0 *3*	0.022 *3*			3227.5
706.01 *8*	0.079 *10*			?
		706.4 *4*	3130 *50*	3097.3
714.4[d] *5*	0.005 *2*	714.4 *5*	3180 *50*	3105.4

TABLE II. (*Continued*).

(n,γ) E_γ (keV)[a]	(n,γ) I_γ (b)	$(n,n'\gamma)$ E_γ (keV)[b]	$(n,n'\gamma)$ E_{th} (keV)[c]	Placement
		731.2 *7*	3200 *300*	3097.3
733.894 *28*	2.1 *4*	734.0 *3*	2070 *30*	2027.5
738.8[d] *5*	0.008 *3*	738.8 *5*	3200 *100*	3105.4
740.18 *16*	0.036 *5*			?
		748.0 *6*	< 4500	3277.3
770.95 *7*	0.063 *7*	770.7 *5*	3100 *200*	2996.3
786.36 *22*	0.019 *4*			?
788.81 *8*	0.063 *7*	789.4 *6*	3220 *70*	3179.7
791.75 *6*	0.104 *11*	791.6 *4*	3200 *50*	3157.9
806.662 *26*	0.32 *5*			?
818.717 *22*	3.0 *3*	818.67 *7*	2110 *20*	2112.3
828.79 *9*	0.070 *9*	828.8 *7*	2600 *150*	2585.6
		831.1 *7*	3100 *80*	3097.3
831.03 *10*	0.121 *14*	831.1 *7*	3400 *70*	3416.6
835.07 *19*	0.021 *4*			4251.7
839.6[d] *5*	0.005 *2*	839.6 *5*	3000 *300*	3105.4
840.14 *11*	0.044 *5*			4211.6
		844.1 *8*	< 3750	3210.1
		849.8 *6*	3250 *200*	?
857.19 *15*	0.066 *10*	857.9 *8*	3780 *100*	3658.7
868.04 *6*	0.108 *12*			3711.9
884.32 *8*	0.084 *11*	884.6 *7*	< 3750	?
		886.2 *7*	3350 *150*	?
891.69 *11*	0.043 *8*	891.5 *4*	3300 *80*	3257.8
924.1 *4*	0.018 *12*	923.9 *7*	3350 *100*	?
931.858 *22*	2.5 *3*	931.78 *10*	2250 *30*	2225.4
		943.1 *4*	3340 *100*	3309.2
961.3 *4*	0.09 *3*	961.5 *6*	3300 *70*	3227.5
961.9 *4*	0.05 *2*	962.0 *6*	3300 *70*	3228.1
972.615 *20*	3.4 *4*	972.59 *10*	2285 *20*	2266.2
980.42 *22*	0.021 *5*	980.3 *10*	3500 *200*	3371.4
1000.92 *12*	0.080 *12*	1001.1 *5*	3700 *100*	3586.6
1002.6 *4*	0.023 *8*			3228.1
1012.85 *28*	0.045 *9*			?
1022.83 *17*	0.035 *5*	1022.7 *6*	3290 *30*	3289.1
1043.70 *14*	0.037 *7*			?
1060.9 *6*	0.03 *1*	1060.9 *6*	3400 *50*	3428.0
1072.48 *8*	0.088 *10*	1072.5 *6*	2400 *150*	2366.1
1078.14 *7*	0.15 *5*	1077.8 *6*	3340 *60*	3344.4
1089.56 *14*	0.07 *3*	1090.0 *4*	3400 *100*	3315.0
1097.327 *22*	0.87 *10*	1097.31 *5*	2395 *20*	2390.9
1115.16 *5*	0.36 *5*	1115.6 *5*	3220 *40*	3227.5
1119.00 *7*	0.16 *3*	1119.2 *6*	3350 *40*	3344.4
1123.68 *6*	0.20 *4*	1123.8 *5*	3270 *40*	3236.0
1136.2 *4*	0.019 *6*			4480.2
1146.03 *22*	0.037 *7*	1145.6 *7*	< 3750	3371.4
1150.31 *6*	0.18 *3*	1150.6 *5*	3440 *40*	3416.6
1161.80 *14*	0.060 *10*	1161.3 *3*	3470 *30*	3428.0
1165.15 *25*	0.058 *9*			4392.6
		1185.3 *6*	3600 *80*	3576.2
		1189.9 *6*	3750 *200*	?
1191.08 *17*	0.041 *9*			3776.8
1200.5 *3*	0.36 *3*	1200.2 *6*	3240 *40*	3228.1
1202.9 *3*	0.29 *4*	1203.1 *4*	3330 *50*	3315.0
1210.6 *7*	0.015 *9*			4001.1
1231.94 *11*	0.067 *10*	1232.0 *7*	< 4500	3344.4
1241.08 *20*	0.058 *9*	1241.0 *7*	3560 *40*	3507.3
1244.25 *12*	0.122 *14*	1243.8 *7*	3530 *30*	3469.7

TABLE II. (*Continued*).

(n,γ) E_γ (keV)[a]	(n,γ) I_γ (b)	$(n,n'\gamma)$ E_γ (keV)[b]	$(n,n'\gamma)$ E_{th} (keV)[c]	Placement
		1249.8 *7*	3670 *40*	3640.7
1252.119 *24*	0.69 *8*	1252.0 *6*	2585 *20*	2545.7
		1257.0 *5*	3670 *50*	3648.1
		1282.5 *8*	3680 *60*	3648.1
1292.0[f] *2*	1.1[f] *2*	1292.0[g] *5*		2585.6
1293.586 *26*	30.1 *30*	1293.58 *5*		1293.6
1303.86 *15*	0.043 *10*			4392.6
1331.68 *10*	0.074 *11*	1331.8 *5*	3060 *80*	3088.6
		1350.1 *4*	3660 *30*	3616.3
1356.851 *22*	1.6 *3*	1356.98 *15*	2680 *20*	2650.5
1368.38 *9*	0.100 *14*	1368.3 *4*	3640 *30*	3593.8
1396.03 *15*	0.088 *16*	1395.8 *5*	3600 *100*	3508.4
1409.66 *17*	0.063 *13*	1408.7 *7*	$<$4500	4200.1
		1421.2 *5*	3850 *60*	3787.3
1433.40 *14*	0.037 *8*	1434.5 *10*	3700 *100*	3658.7
		1440.7 *7*	$<$4200	3706.9
1460.67 *10*	0.064 *10*	1460.8 *7*	$<$4500	?
1474.45 *19*	0.089 *15*	1474.5 *8*	3700 *100*	3586.6
1476.75 *19*	0.091 *14*	1476.3 *4*	3780 *30*	3743.0
1481.4 *4*	0.036 *7*	1481.4 *5*	3650 *100*	3593.8
1496.91 *6*	0.18 *3*	1496.7 *4*	2850 *40*	2790.6
1507.66 *5*	0.25 *4*	1507.70 *10*	2800 *50*	2801.4
1517.94 *28*	0.028 *5*			4308.5
1546.42 *7*	0.21 *4*	1547.0 *7*	3700 *40*	3658.7
1550.0 *3*	0.23 *8*	1550.3 *5*	2850 *30*	2843.8
1551.3 *6*	0.13 *8*			4201.5
1568.02 *20*	0.026 *7*			4113.9
1576.74 *21*	0.037 *9*	1577.3 *8*	4200 *200*	4162.4
1584.1 *6*	0.016 *6*			3851.0
1586.43 *27*	0.035 *7*			4430.5
1616.06 *14*	0.105 *14*			4201.5
1618.7 *6*	0.022 *8*	1618.0 *7*	3900 *100*	3843.7
1631.0[d] *10*	0.048 *8*	1631.0 *10*	3900 *150*	3743.0
1650.74 *6*	0.19 *3*	1650.8 *4*	3970 *40*	3917.0
1666.38 *7*	0.23 *3*	1666.1 *4*	2970 *40*	2960.1
1671.3 *5*	0.028 *10*			?
1678.2 *3*	0.032 *7*	1678.0 *7*	$<$4500	3903.6
1684.6[d] *8*	0.010 *5*	1684.6 *8*	4000 *150*	3950.3
		1693.1 *8*	3950 *100*	3805.5
		1697.0 *8*	3950 *150*	3809.3
1702.68 *5*	0.32 *5*	1702.5 *2*	3025 *30*	2996.3
1711.16 *9*	0.35 *5*			5055.6
1724.58 *30*	0.037 *7*	1724.7 *5*	3850 *150*	3950.3
1731.8 *4*	0.027 *7*	1731.4 *5*	3750 *150*	3843.7
1752.72 *12*	0.103 *11*	1752.6 *3*	3080 *30*	3046.4
1771.2 *5*	0.035 *7*	1770.4 *6*	$<$4500	4037.4
1787.54 *25*	0.037 *7*			4013.2
1795.02 *7*	0.131 *17*	1795.1 *6*	3120 *30*	3088.6
1860.44 *28*	0.061 *9*			4511.5
		1861.4 *8*	4000 *150*	3973.7
1863.5 *4*	0.049 *9*			4392.6
1870.8 *5*	0.036 *11*			9563.5
1877.36 *8*	0.23 *3*	1877.5 *5*	3900 *80*	3904.9
1882.9 *7*	0.045 *14*			4411.0
1886.12 *10*	0.24 *5*	1886.0 *3*	3210 *30*	3179.7
1896.49 *19*	0.083 *11*	1896.0 *6*	4000 *200*	4162.4
1900.72 *5*	0.44 *9*	1901.0 *5*	3230 *30*	3194.3
		1902.7 *8*	4150 *200*	4015.1

TABLE II. (*Continued*).

(n,γ) E_γ (keV)[a]	(n,γ) I_γ (b)	$(n,n'\gamma)$ E_γ (keV)[b]	$(n,n'\gamma)$ E_{th} (keV)[c]	Placement
1903.88 *29*	0.074 *11*			9563.5
1924.3 *6*	0.031 *13*			4190.5
1926.3 *4*	0.051 *15*			4511.5
1934.52 *21*	0.074 *22*	1934.1 *5*	3230 *60*	3228.1
1935.46 *22*	0.114 *23*			4201.5
1942.51 *13*	0.054 *11*			3236.0
1963.67 *23*	0.058 *10*	1963.1 *4*	4200 *150*	4076.0
1972.82 *19*	0.081 *12*	1973.2 *7*	4200 *200*	?
1976.06 *9*	0.19 *4*	1976.2 *9*	<4500	4201.5
2001.76 *29*	0.045 *9*			4392.6
		2014.5 *7*	4300 *150*	4280.7
2021.3 *5*	0.05 *2*	2021.3 *8*	3400 *150*	3315.0
2050.4 *7*	0.15 *8*	2050.9 *4*	3370 *40*	3344.4
2051.5 *7*	0.22 *7*			5395.5
2077.82 *10*	0.120 *17*	2077.7 *4*	3390 *30*	3371.4
2112.313 *22*	3.4 *4*	2112.24 *8*	2120 *20*	2112.3
2122.3 *7*	0.15 *3*	2122.6 *6*	3410 *60*	3415.9
2148.06 *6*	0.25 *4*	2148.0 *5*	4000 *70*	3904.9
2175.89 *13*	0.13 *2*	2175.9 *4*	3490 *30*	3469.7
2211.72 *11*	0.13 *2*			5055.6
2220.1[d] *6*	0.41 *10*	2220.1 *6*	3590 *40*	3513.6
2225.4 *5*	1.1 *3*	2225.2 *5*	2280 *40*	2225.4
2244.21 *7*	0.23 *3*	2243.8 *4*	4030 *70*	4001.1
2254.72 *24*	0.088 *13*			4480.2
2258.1 *5*	0.053 *9*	2258.4 *5*	3630 *70*	3551.7
2271.59 *28*	0.053 *9*			?
2275.6 *6*	0.037 *8*			4925.9
2279.16 *17*	0.141 *18*	2279.5 *3*	3600 *20*	3572.9
2282.35 *29*	0.067 *11*			5242.3
2291.68 *25*	0.061 *9*			4877.2
2301.62 *26*	0.066 *10*			4952.1
		2331.0 *7*	3670 *70*	3624.6
2357.01 *6*	0.24 *3*	2356.9 *7*	4100 *100*	4113.9
2402.2 *7*	0.084 *24*			4430.5
2437.0 *4*	0.100 *30*	2437.3 *7*	3750 *50*	3730.6
2449.0[d] *5*	0.040 *6*	2449.0 *5*	3800 *100*	3743.0
2454.3 *4*	0.067 *25*	2454.5 *5*	3800 *50*	3747.9
		2511.9 *6*	3900 *80*	3805.5
2529.2 *5*	0.054 *16*			9563.5
2535.9 *5*	0.035 *15*			4649.2
2543.06 *23*	0.099 *18*	2542.9 *8*	3850 *100*	3836.7
2549.85 *22*	0.122 *22*	2549.7 *3*	3870 *30*	3843.7
2585.66 *8*	0.73 *10*	2585.9 *2*	2640 *40*	2585.6
2620.7 *6*	0.10 *4*			4649.2
2650.4 *5*	0.12 *2*	2650.6 *8*	2720 *60*	2650.5
2652.2 *5*	0.16 *3*	2652.6 *9*	3980 *40*	3945.8
2657.4[d] *7*	0.008 *4*	2657.4 *7*	4000 *100*	3950.3
2707.48 *22*	0.18 *4*	2707.4 *4*	4100 *100*	4001.1
2719.7 *4*	0.10 *4*	2719.1 *9*	4100 *100*	4013.2
		2721.5 *9*	4200 *150*	4015.1
2734.9 *5*	0.070 *23*	2734.8 *6*	<4500	4028.5
2743.5 *4*	0.11 *4*	2742.8 *3*	4100 *100*	4037.4
2754.67 *27*	0.18 *4*			4511.5
2843.85 *7*	0.74 *10*	2843.9 *2*	2860 *20*	2843.8
2850.3 *5*	0.099 *20*	2850.0 *6*	4100 *100*	4143.9
2868.48 *20*	0.18 *4*	2868.2 *5*	4100 *100*	4162.4
2877.5 *4*	0.085 *18*	2877.1 *7*	<4500	4170.9
2896.9 *4*	0.084 *19*	2897.1 *7*	4200 *200*	4190.5

TABLE II. (*Continued*).

(n,γ) E_γ (keV)[a]	(n,γ) I_γ (b)	$(n,n'\gamma)$ E_γ (keV)[b]	$(n,n'\gamma)$ E_{th} (keV)[c]	Placement
2907.2 *5*	0.059 *17*			4201.5
2918.07 *22*	0.18 *4*	2918.2 *5*	4200 *200*	4211.6
2944.5[g] *3*	0.10[g] *3*			6041.8
2944.8[g] *3*	0.06[g] *2*	2945.2 *6*	4200 *200*	4238.5
2960.06 *8*	0.45 *7*	2959.8 *3*	3000 *20*	2960.1
2977.2 *4*	0.09 *3*			5562.8
2984.70 *23*	0.18 *3*	2985.1 *6*	4200 *200*	4278.4
3003.5 *5*	0.075 *17*	3003.2 *5*	<4500	4297.1
3008.2 *5*	0.05 *2*			5968.5
3015.1 *5*	0.051 *12*			4308.5
3026.8 *6*	0.048 *15*			6116.6
3088.47 *11*	0.38 *5*	3088.5 *2*	3140 *40*	3088.6
3095.1 *4*	0.11 *3*			9563.5
3099.31 *30*	0.15 *3*			4392.6
3117.6 *5*	0.086 *16*			4411.0
3127.73 *27*	0.106 *17*			9563.5
3132.7 *6*	0.06 *2*			5357.9
3141.4 *7*	0.063 *17*			?
3157.88 *17*	0.14 *3*			9563.5
3186.55 *12*	0.17 *3*			4480.2
3296.7 *4*	0.07 *3*			5562.8
3309.4 *4*	0.09 *3*			5066.2
3331.0 *7*	0.35 *9*			5357.9
3333.73 *6*	1.21 *14*	3333.6 *4*	3370 *20*	3333.8
3351.4 *5*	0.09 *2*			6532.1
3356.5 *6*	0.048 *12*			4649.2
3393.8 *4*	0.06 *2*			6482.6
3403.92 *11*	0.24 *3*			9563.5
3411.2 *4*	0.047 *13*			9563.5
3417.6 *5*	0.033 *12*			5174.4
3456.68 *22*	0.10 *1*			5484.3
3491.2 *6*	0.06 *3*			5716.4
3500.42 *29*	0.15 *2*			5767.2
3514.0 *5*	0.11 *3*	3514.7 *6*	3560 *50*	3513.6
3521.4 *7*	0.05 *2*			6482.6
3528.8 *4*	0.06 *2*			6373.0
3549.0 *4*	0.074 *16*			6198.7
3554.5 *7*	0.06 *2*			5667.8
3558.9 *5*	0.08 *2*			4852.7
3567.9 *4*	0.07 *2*			9563.5
3574.06 *19*	0.17 *3*			9563.5
3578.1 *7*	0.026 *11*			5968.5
3586.83 *22*	0.11 *1*	3586.9 *4*	4000 *400*	3586.6
3592.83 *28*	0.10 *1*			6436.2
3598.4 *5*	0.076 *13*			4892.6
3626.7 *5*	0.04 *1*			6428.1
3632.26 *20*	0.122 *15*			4925.9
3637.0 *4*	0.065 *12*			6428.1
3646.6 *6*	0.02 *1*			6436.2
3650.4 *8*	0.034 *13*			6041.8
3658.3[h] *3*	0.18[h] *4*			4952.1
3658.5[h] *3*	0.18[h] *4*	3658.2 *3*	3710 *40*	3658.7
3677.7 *4*	0.057 *12*			6468.6
3712.06 *16*	0.24 *5*	3711.9 *3*	3740 *30*	3711.9
3720.5 *6*	0.07 *2*			6510.6
3740.6 *6*	0.035 *15*			5767.2
3764.8 *6*	0.042 *12*			5989.5
3777.1 *3*	0.12 *2*	3777.2 *7*	3850 *200*	3776.8

TABLE II. (*Continued*).

(n,γ) E_γ (keV)[a]	(n,γ) I_γ (b)	$(n,n'\gamma)$ E_γ (keV)[b]	$(n,n'\gamma)$ E_{th} (keV)[c]	Placement
3793.6 *6*	0.03 *1*			6754.1
3805.95 *18*	0.12 *2*	3805.9 *5*	3850 *70*	3806.0
3811.2 *6*	0.03 *1*			5923.6
3816.3 *3*	0.10 *3*			6041.8
3832.3 *6*	0.04 *1*			6482.6
3842.6 *4*	0.07 *2*			6428.1
3848.1 *6*	0.03 *2*			9563.5
3852.0 *8*	0.04 *2*	3851.8 *9*	3900 *100*	3851.0
3855.6 *8*	0.04 *2*			5968.5
3859.9 *8*	0.03 *2*			6510.6
3876.8 *4*	0.060 *10*			5989.5
3896.0 *4*	0.064 *12*			9563.5
3903.5 *4*	0.12 *2*	3904.4 *7*	4100 *300*	3903.6
3911.6 *4*	0.057 *12*			5667.8
3926.4 *6*	0.02 *1*			6152.1
3932.5 *4*	0.08 *2*			6198.7
3938.0 *5*	0.04 *1*			7173.9
3947.9 *6*	0.04 *1*			5242.3
3952.5 *4*	0.063 *11*	3951.9 *6*	4050 *100*	3952.9
3968.18 *20*	0.18 *3*			5995.6
4000.4 *4*	0.06 *2*			9563.5
4013.4 *2*	0.35 *4*	4013.6 *3*	4050 *50*	4013.2
4026.5 *3*	0.13 *2*	4026.8 *7*	4050 *100*	4026.8
4064.0 *3*	0.13 *2*			5357.9
4070.7 *5*	0.06 *2*			9563.5
4076.9 *6*	0.040 *11*			6468.6
4092.4 *4*	0.14 *3*			6482.6
4101.8 *3*	0.13 *2*			5395.5
4113.9 *2*	0.17 *3*			4113.9
4128.2 *2*	0.26 *4*	4129.3 *8*	4200 *200*	4128.3
4135.8 *4*	0.13 *4*			7224.7
4162.4 *6*	0.10 *3*			6428.1
4170.4 *6*	0.07 *2*	4170.2 *8*	<4500	4170.9
4181.5 *3*	0.15 *3*			5474.9
4199.79 *22*	0.12 *2*	4198.9 *5*	4200 *200*	4200.1
4209.8 *5*	0.046 *13*			6436.2
4237.83 *27*	0.06 *2*	4237.5 *10*	<4500	4238.5
4246.1 *5*	0.043 *10*			6357.7
4251.64 *12*	0.16 *3*	4251.7 *5*	<4500	4251.7
4257.5 *7*	0.04 *1*			6482.6
4268.85 *27*	0.15 *3*			5562.8
4279.0 *4*	0.036 *11*	4278.6 *8*	<4500	4278.4
4293.18 *15*	0.18 *3*			6405.6
4306.74 *25*	0.13 *2*			6532.1
4321.1 *4*	0.03 *1*			9563.5
4360.1 *5*	0.053 *12*			6116.6
4374.15 *20*	0.16 *3*			6131.0
4392.54 *12*	0.32 *5*			4392.6
4410.81 *16*	0.13 *4*			4411.0
4423.0 *4*	0.14 *2*			5716.4
4431.0 *4*	0.08 *2*			4430.5
4441.68 *11*	0.28 *4*			6198.7
4449.50 *12*	0.22 *3*			7035.0
4473.57 *12*	0.19 *3*			5767.2
4483.12 *23*	0.16 *3*			6510.6
4497.3 *3*	0.048 *12*			9563.5
4511.2 *4*	0.11 *3*			4511.5
4548.28 *14*	0.17 *3*			4548.5

TABLE II. (*Continued*).

(n,γ) E_γ (keV)[a]	(n,γ) I_γ (b)	$(n,n'\gamma)$ E_γ (keV)[b]	$(n,n'\gamma)$ E_{th} (keV)[c]	Placement
4584.03 *24*	0.10 *1*			4584.0
4600.4 *3*	0.07 *2*			6357.7
4611.2 *5*	0.03 *1*			9563.5
4629.9 *3*	0.05 *1*			5923.6
4641.5 *2*	0.09 *2*			6754.1
4649.15 *10*	0.20 *2*			4649.2
4670.8 *6*	0.05 *2*			9563.5
4674.6 *3*	0.113 *19*			7325.3
4685.9 *3*	0.067 *11*			9563.5
4695.85 *10*	0.65 *7*			5989.5
4701.85 *12*	0.25 *3*			5995.6
4712.7 *5*	0.053 *9*			6468.6
4725.6 *3*	0.08 *2*			6482.6
4769.4 *10*	0.09 *5*			7035.0
4780.2 *15*	0.05 *4*			7325.3
4809.42 *10*	0.35 *4*			7035.0
4816.1 *3*	0.063 *9*			7659.9
4823.0 *3*	0.05 *1*			6116.6
4837.0 *3*	0.052 *11*			6131.0
4852.6 *3*	0.08 *2*			4852.7
4858.2 *4*	0.068 *11*			6152.1
4865.97 *11*	0.21 *2*			6159.6
4876.88 *17*	0.123 *18*			4877.2
4892.54 *22*	0.075 *11*			4892.6
4905.9 *5*	0.037 *10*			6198.7
4914.31 *13*	0.26 *2*			9563.5
4925.8 *2*	0.13 *2*			4925.9
4934.0 *4*	0.057 *12*			7325.3
4959.7 *3*	0.136 *19*			6717.3
4979.51 *18*	0.112 *16*			9563.5
5014.3 *4*	0.08 *2*			9563.5
5051.0 *5*	0.033 *8*			9563.5
5062.1 *8*	0.024 *6*			7173.9
5066.2 *6*	0.03 *1*			5066.2
5079.6 *4*	0.07 *2*			6373.0
5083.33 *17*	0.23 *3*			9563.5
5114.1 *3*	0.058 *11*			7659.9
5134.2 *6*	0.03 *1*			7246.4
5142.2 *4*	0.044 *12*			6436.2
5152.4 *2*	0.092 *20*			9563.5
5170.4 *6*	0.14 *8*			9563.5
5172.9 *20*	0.09 *5*			5174.4
5176.4 *15*	0.033 *9*			6468.6
5188.4 *4*	0.048 *10*			6482.6
5216.8 *1*	0.15 *2*			6510.6
5238.4 *6*	0.036 *8*			6532.1
5255.5 *6*	0.024 *7*			9563.5
5268.8 *4*	0.03 *1*			7659.9
5285.4 *3*	0.060 *11*			9563.5
5298.4 *5*	0.08 *2*			7325.3
5311.5 *3*	0.09 *2*			9563.5
5324.71 *16*	0.15 *2*			9563.5
5352.0 *3*	0.064 *10*			9563.5
5361.99 *10*	0.72 *9*			9563.5
5401.1 *3*	0.07 *2*			9563.5
5416.3 *6*	0.03 *1*			7173.9
5423.60 *11*	0.43 *5*			6717.3
5427.8 *7*	0.06 *2*			7692.8
5449.46 *10*	0.40 *4*			9563.5
5461.1 *4*	0.08 *2*			6754.1

TABLE II. (*Continued*).

(n,γ) E_γ (keV)[a]	(n,γ) I_γ (b)	$(n,n'\gamma)$ E_γ (keV)[b]	$(n,n'\gamma)$ E_{th} (keV)[c]	Placement
5467.1 *2*	0.10 *1*			7692.8
5474.0 *5*	0.04 *1*			5474.9
5484.5 *9*	0.03 *1*			5484.3
5488.6 *20*	0.02 *1*			9563.5
5493.1 *6*	0.051 *12*			5493.0
5525.6 *5*	0.03 *1*			9563.5
5536.5 *3*	0.06 *2*			9563.5
5550.39 *14*	0.23 *3*			9563.5
5562.38 *10*	0.34 *4*			9563.5
5580.6 *5*	0.05 *1*			7692.8
5610.6 *7*	0.036 *9*			9563.5
5646.48 *16*	0.11 *3*			9563.5
5658.6 *3*	0.09 *3*			9563.5
5659.8 *5*	0.05 *2*			9563.5
5757.5 *4*	0.03 *1*			9563.5
5787.0 *6*	0.04 *1*			9563.5
5851.55 *23*	0.066 *10*			9563.5
5904.84 *10*	0.46 *4*			9563.5
5931.4 *6*	0.03 *1*			7224.7
5952.3 *6*	0.03 *1*			7246.4
5969.2 *6*	0.054 *9*			9563.5
5977.6 *5*	0.05 *2*			9563.5
6054.95 *20*	0.12 *2*			9563.5
6093.04 *30*	0.11 *3*			9563.5
6109.3 *6*	0.03 *1*			?
6146.7 *2*	0.08 *2*			9563.5
6158.96 *24*	0.059 *10*			6159.6
6229.50 *10*	0.34 *4*			9563.5
6248.4 *6*	0.03 *1*			9563.5
6335.87 *11*	0.32 *5*			9563.5
6475.7 *5*	0.05 *1*			9563.5
6603.3 *11*	0.38 *5*			9563.5
6718.9 *5*	0.03 *1*			9563.5
6772.9 *5*	0.022 *5*			9563.5
6913.07 *17*	0.10 *1*			9563.5
6978.03 *26*	0.04 *1*			9563.5
7017.55 *10*	0.23 *3*			9563.5
7337.72 *15*	0.15 *2*			9563.5
7450.76 *11*	0.29 *4*			9563.5
7806.4 *5*	0.022 *3*			9563.5
8269.56 *25*	0.045 *7*			9563.5
9562.8 *5*	0.055 *11*			9563.5

[a]The notation, 99.9 *5*, denotes 99.5±0.5 keV, etc.

[b]Energy calibration taken from strong transitions in ^{115}Sn(n,γ).

[c]Threshold energy is obtained from a linear extrapolation of $I_\gamma(E_n)$ to zero intensity. This E_{th} is typically 30–100 keV higher than E(level).

[d]γ ray not observed in the (n,γ) experiment; intensity inferred from measured branching in the $(n,n'\gamma)$ experiment or from the literature.

[e]The measured energy and intensity for this composite peak were 416.936 *20* and 0.47 *10*, respectively. The energy 416.86 keV is from Ref. 36 and the energy 417.4 keV is deduced from the level scheme. The intensity of the 417.4-keV γ ray was inferred from the measured branching in the $(n,n'\gamma)$ reaction.

[f]Inferred from the excitation function of 2586G [see Fig. 5(a)] and comparison with calculated statistical model cross sections.

[g]The measured energy and intensity for this composite peak were 2944.66 *19* and 0.16 *3*, respectively. The intensity of the 2944.8-keV γ ray was inferred from the measured branching in the $(n,n'\gamma)$ reaction.

[h]The measured energy and intensity for this composite peak were 3658.39 *10* and 0.36 *5*, respectively. The intensity of the 3658.5-keV γ ray was inferred from the measured branching in the $(n,n'\gamma)$ reaction.

TABLE III. Level scheme in tabular form of ^{116}Sn from the ^{115}Sn(n,γ) and ^{116}Sn(n,n'γ) reactions.

Level energy[a] (keV)	Deexciting γ rays[b] (keV)	Level energy[a] (keV)	Deexciting γ rays[b] (keV)
0.0		3658.69 *6*	3658.5, 1546.42, 1433.40, 857.19
1293.605 *17*	1293.586	3706.9 *7*	1440.7
1756.849 *23*	463.249	3711.91 *7*	3712.06, 868.04
2027.50 *4*	733.894	3730.6 *4*	2437.0
2112.332 *17*	2112.313, 818.717, 355.492	3742.96 *18*	2449.0, 1631.0, 1476.75
2225.447 *24*	2225.4, 931.858	3747.9 *4*	2454.3
2266.228 *24*	972.615	3776.79 *15*	3777.1, 1191.08
2366.11 *8*	1072.48, 99.9	3787.3 *5*	1421.2
2390.92 *3*	1097.327	3805.5 *6*	2511.9, 1693.1
2529.25 *4*	416.86, 138.39	3806.00 *17*	3805.95
2545.74 *3*	1252.119, 433.90	3809.3 *8*	1697.0
2585.61 *3*	2585.66, 1292.0, 828.79, 360.173	3836.69 *23*	2543.06
2650.47 *3*	2650.4, 1356.851, 538.21, 384.22	3843.69 *19*	2549.85, 1731.8, 1618.7
2773.55 *13*	407.43	3851.0 *5*	3852.0, 1584.1
2790.57 *4*	1496.91, 678.28, 565.16, 204.96	3903.62 *22*	3903.5, 1678.2
2801.35 *5*	1507.66	3904.91 *6*	2148.06, 1877.36
2843.84 *5*	2843.85, 1550.0, 577.36	3916.97 *6*	1650.74
2909.6 *5*	543.5	3945.8 *5*	2652.2
2960.07 *4*	2960.06, 1666.38, 693.82, 374.52, 309.75	3950.3 *3*	2657.4, 1724.58, 1684.6
2996.29 *4*	1702.68, 770.95, 605.34, 466.7, 194.83	3952.9 *3*	3952.5, 439.32
3016.58 *12*	650.46	3973.7 *8*	1861.4
3032.2 *4*	641.1, 503.3	4001.07 *6*	2707.48, 2244.21, 1210.6
3046.41 *10*	1752.72, 655.60	4013.16 *11*	4013.4, 2719.7, 1787.54
3088.63 *5*	3088.47, 1795.02, 1331.68	4015.1 *6*	2721.5, 1902.7
3097.28 *23*	831.1, 731.2, 706.4, 568.0	4026.75 *22*	4026.5
3105.35 *18*	839.6, 738.8, 714.4, 331.80	4028.5 *5*	2734.9
3157.87 *10*	791.75	4037.4 *3*	2743.5, 1771.2
3179.72 *6*	1886.12, 788.81, 378.24	4076.03 *20*	1963.67, 417.4
3194.34 *6*	1900.72	4113.90 *6*	4113.9, 2357.01, 1568.02
3210.1 *5*	844.1, 436.5	4128.28 *20*	4128.2
3227.47 *5*	1115.16, 961.3, 698.0, 641.63	4143.9 *5*	2850.3
3228.10 *15*	1934.52, 1200.5, 1002.6, 961.9	4162.41 *11*	2868.48, 1896.49, 1576.74
3236.04 *6*	1942.51, 1123.68	4170.9 *4*	4170.4, 2877.5
3257.81 *14*	891.69	4190.5 *4*	2896.9, 1924.3
3277.3 *6*	748.0	4200.10 *14*	4199.79, 1409.66
3289.06 *18*	1022.83	4201.53 *6*	2907.2, 1976.06, 1935.46, 1616.06, 1551.3
3309.2 *4*	943.1, 535.5	4211.59 *11*	2918.07, 840.14
3315.04 *13*	2021.3, 1202.9, 1089.56	4238.50 *13*	4237.83, 2944.8
3333.81 *6*	3333.73	4251.73 *10*	4251.64, 835.07
3344.39 *5*	2050.4, 1231.94, 1119.00, 1078.14, 500.84	4278.38 *17*	4279.0, 2984.70
3350.6 *4*	549.1, 355.0	4280.7 *7*	2014.5
3371.44 *8*	2077.82, 1146.03, 980.42	4297.1 *5*	3003.5
3415.9 *7*	2122.3	4308.48 *23*	3015.1, 1517.94
3416.58 *6*	1150.31, 831.03	4392.63 *8*	4392.54, 3099.31, 2001.76, 1863.5, 1303.86, 1165.15
3427.98 *14*	1161.80, 1060.9		
3453.9 *4*	407.5	4411.01 *12*	4410.81, 3117.6, 1882.9
3469.71 *9*	2175.89, 1244.25, 668.5, 125.66	4430.46 *22*	4431.0, 2402.2, 1586.43
3507.31 *21*	1241.08	4480.19 *9*	3186.55, 2254.72, 1136.2
3508.36 *7*	1396.03, 664.54, 548.34, 419.60	4511.47 *16*	4511.2, 2754.67, 1926.3, 1860.44
3513.6 *3*	3514.0, 2220.1	4548.46 *14*	4548.28
3551.7 *5*	2258.1	4584.00 *15*	4584.03
3572.89 *11*	2279.16	4649.19 *8*	4649.15, 3356.5, 2620.7, 2535.9
3576.2 *6*	1185.3	4852.7 *3*	4852.6, 3558.9
3586.63 *10*	3586.83, 1474.45, 1000.92	4877.18 *13*	4876.88, 2291.68
3593.84 *9*	1481.4, 1368.38	4892.57 *19*	4892.54, 3598.4
3616.3 *4*	1350.1	4925.93 *14*	4925.8, 3632.26, 2275.6
3624.6 *7*	2331.0	4952.08 *19*	3658.3, 2301.62
3640.7 *7*	1249.8	5055.57 *8*	2211.72, 1711.16
3648.1 *5*	1282.5, 1257.0	5066.23 *23*	5066.2, 3309.4

TABLE III. *(continued)*

Level energy[a] (keV)	Deexciting γ rays[b] (keV)	Level energy[a] (keV)	Deexciting γ rays[b] (keV)
5174.4 *5*	5172.9, 3417.6	6482.60 *17*	5188.4, 4725.6, 4257.5, 4092.4, 3832.3,
5242.31 *22*	3947.9, 2282.35		3521.4, 3393.8
5357.9 *3*	4064.0, 3331.0, 3132.7	6510.57 *10*	5216.8, 4483.12, 3859.9, 3720.5
5395.5 *3*	4101.8, 2051.5	6532.06 *21*	5238.4, 4306.74, 3351.4
5474.9 *3*	5474.0, 4181.5	6717.26 *11*	5423.60, 4959.7
5484.26 *22*	5484.5, 3456.68	6754.08 *18*	5461.1, 4641.5, 3793.6
5493.0 *4*	5493.1	7035.05 *8*	4809.42, 4769.4, 4449.50
5562.79 *18*	4268.85, 3296.7, 2977.2	7173.9 *4*	5416.3, 5062.1, 3938.0
5667.8 *3*	3911.6, 3554.5	7224.7 *4*	5931.4, 4135.8
5716.4 *3*	4423.0, 3491.2	7246.4 *5*	5952.3, 5134.2
5767.22 *11*	4473.57, 3740.6, 3500.42	7325.31 *22*	5298.4, 4934.0, 4780.2, 4674.6
5923.6 *3*	4629.9, 3811.2	7659.88 *16*	5268.8, 5114.1, 4816.1
5968.5 *4*	3855.6, 3578.1, 3008.2	7692.82 *17*	5580.6, 5467.1, 5427.8
5989.53 *9*	4695.85, 3876.8, 3764.8	9563.56 *3*	9562.8, 8269.56, 7806.4, 7450.76, 7337.72,
5995.61 *11*	4701.85, 3968.18		7017.55, 6978.03, 6913.07, 6772.9, 6718.9,
6041.79 *24*	3816.3, 3650.4, 2944.5		6603.3, 6475.7, 6335.87, 6248.4, 6229.50,
6116.59 *24*	4823.0, 4360.1, 3026.8		6146.7, 6093.04, 6054.95, 5977.6, 5969.2,
6130.97 *17*	4837.0, 4374.15		5904.84, 5851.55, 5787.0, 5757.5, 5659.8,
6152.1 *3*	4858.2, 3926.4		5658.6, 5646.48, 5610.6, 5562.38, 5550.39,
6159.59 *8*	6158.96, 4865.97		5536.5, 5525.6, 5488.6, 5449.46, 5401.1,
6198.73 *11*	4905.9, 4441.68, 3932.5, 3549.0		5361.99, 5352.0, 5324.71, 5311.5, 5285.4,
6357.7 *3*	4600.4, 4246.1		5255.5, 5170.4, 5152.4, 5083.33, 5051.0,
6373.0 *3*	5079.6, 3528.8		5014.3, 4979.51, 4914.31, 4685.9, 4670.8,
6405.61 *12*	4293.18		4611.2, 4497.3, 4321.1, 4070.7, 4000.4,
6428.10 *23*	4162.4, 3842.6, 3637.0, 3626.7		3896.0, 3848.1, 3574.06, 3567.9, 3411.2,
6436.17 *16*	5142.2, 4209.8, 3646.6, 3592.83		3403.92, 3157.88, 3127.73, 3095.1, 2529.2,
6468.61 *23*	5176.4, 4712.7, 4076.9, 3677.7		1903.88, 1870.8

[a]The notation, 1293.605 *17* denotes 1293.605 ± 0.017 keV, etc.
[b]See Tables II and IV for the appropriate intensity values.

$$\sigma_{ab} = \sigma_a P_b = \pi \lambda_a^2 T_a \left[T_b \Big/ \sum T_c \right] W_{ab} ,$$

where T_i are transmission coefficients calculated with an optical-model potential that gives a good fit to the total cross section and the differential elastic-scattering cross section, and W_{ab} is a correction factor for the effect of width fluctuations and channel correlations between neutron-scattering channels. (The summations over the appropriate angular momenta have been suppressed in the above schematic equation. See Refs. 52–55 for details.) The rising part of the excitation function [see Fig. 4(a)] is determined mainly by the penetrability for the incident neutrons, while the flat or falling part depends on the way in which competing exit channels open up with increasing energy. The rising part usually extrapolates to zero within 30 keV of threshold for strong decays. For weaker decays, offsets of ~ 150 keV were noted. The energy region over which the curve rises to its maximum value generally increases with increasing spin of the level being excited,[56–58] though this spin dependence is more pronounced in the $A = 190$ region than it is here.

The excitation functions of γ rays depopulating levels that are strongly fed by γ decays from higher-lying states have a much different appearance from those without such feeding. Typical examples of the effect of feeding are shown in Figs. 4(b)–4(d). For instance, the cross section of the 1097-keV γ ray in Fig. 4(b) rises continuously above 3 MeV neutron energy, whereas it might have been expected, in the absence of feeding from above, to reach a maximum at about that point. The excitation function of the 932-keV γ ray in Fig. 4(c) does reach a maximum at 2.9 MeV, and after a minimum at 3.4 MeV, rises again due to γ-ray feeding from higher levels. The data points in these three figures show the measured cross sections of each of three γ rays, and the dashed lines show the graphical subtraction of the cross sections for the γ rays that feed the level. The dot-dashed lines show the inferred cross section for population of the level directly by inelastic neutron scattering. In each case, the inferred cross section shows the typical decreasing straight-line behavior shown by the 2546-keV, low-spin state in Fig. 4(a). Such subtractions have been done for many excitation functions with similar good results in most cases, giving confidence that almost all of the significant decay strength has been measured and the γ rays have been placed correctly in the decay scheme. The only notable discrepancy is the missing feeding [see Fig. 4(b)] to the 2391-keV level (2391L) above 4 MeV neutron energy. (For brevity, the notations "2391L" for the "2391-keV level" and "1293G" for "the 1293-keV γ ray" are adopted in the following discussion.)

The inferred cross section for excitation of 2586L [see Fig. 5(a)] has a quite unreasonable shape, falling almost to zero at 4 MeV and changing slope at that energy. In past experiments (see, for example, Ref. 46) as well as in the current one, it has been found that for most of the levels the inferred cross sections agree quite well with those calculated from the statistical model.[52–55] For this particular level, however, the inferred cross sections at $E_n = 4.5$ MeV is less than 5% of the calculated value. Both of these pieces of evidence imply that ~50% of the decay strength from this level has not been observed. The 2586L has a spin $J = 1$, and there is the possibility of a 40-keV dipole transition to 2546L. This is rejected because the intensity of such a transition would be about twice the total decay intensity of 2546L. The other possibility is that a 1292.0-keV decay occurs to the first-excited state. To get a reasonable cross section for 2586L, this γ ray would have to be only 2% of the intensity of 1293.58G from the 2_1^+ level to the ground state. With such a low relative intensity, a possible 1292.0G would not be detectable in the low-energy tail of 1293.58G. The placement of a 1292.0G between 2586L and 1293L is consistent with the intensity balance for the 1293L final state.

TABLE IV. Branching ratios from the ^{116}Sn$(n,n'\gamma)$ reaction for selected levels. For all other levels observed in this work, the branching ratios can be deduced from Tables II and III.

E(level) (keV)	J^π	Deexciting E_γ (keV)	Branching[a]
3032.2 *4*	6^+	641.1	100
		503.3	82±12
3097.28 *23*	4^+	831.1	24±2
		731.2	21±2
		706.4	100
		568.0	43±4
3105.35 *18*	5^-	839.6	44±6
		738.8	77±3
		714.4	50±5
		331.8	100
3210.1 *5*	7^-	844.1	100
		436.5	40±6
3309.2 *4*	6^-	943.1	100
		535.5	57±11
3350.6 *4*	(5^+)	549.1	100
		355.0	15±3
3648.1 *5*	$3^-,5^-$	1282.5	100
		1257.0	93±10
3742.96 *18*	$1^-,2^+,3^-$	2449.0	42±8
		1631.0	53±10
		1476.3	100
3805.5 *6*	<5	2511.9	100
		1693.1	38±12
3950.3 *3*	$1^-,2,3$	2657.4	24±4
		1724.7	100
		1684.6	28±5
4015.1 *6*	$2,3,4^+$	2721.5	74±9
		1902.7	100
4076.03 *20*	$1^+,2,3$	1963.1	47±16
		417.4	100
4238.50 *13*	2^+	4237.5	93±15
		2945.2	100

[a]Normalized to 100 for the strongest γ ray out of the level.

Another type of departure from the standard shapes shown in Fig. 4(a) results from having two or more γ rays with the same energy (within the experimental resolution) that decay from different levels. An example is seen in the 355G excitation function [Fig. 5(b)], where a second threshold is evident at $E_n = 3.3$ MeV. Between $E_n = 2.75$ MeV and $E_n = 3.75$ MeV, the cross section of 355G increases by about 15%. This increase cannot be due to feeding to 2112L because neither of the other decays from this level, 2112G [see Fig. 5(c)] or 819G [see Fig. 4(d)], show a similar increase. The cross sections for both of these γ rays actually decrease by approximately 15% between $E_n = 2.75$ MeV and $E_n = 3.75$ MeV. Therefore, the existence of a genuine second threshold implies the presence of a second 355G. This transition has been placed as a decay from 3551L. Second thresholds are observed also for the γ rays at 407, 417, 831, and 1901 keV (see below for more details on 407G and 1901G).

Similar behavior occurs when a γ decay has the same energy as the single-escape or double-escape peak of a higher-energy γ ray. An illustrative case is shown in Fig. 5(c). The double-escape peak of 2112G is not resolvable from 1090G, whose existence is established by the threshold at about 3.3 MeV. No such threshold occurs in the 2112G excitation function shown in the same figure. Similar energy coincidences between an escape peak and a real γ ray were observed for the γ rays of 1203.1, 1257.0, 1631.0, 1684.6, 1697.0, 1896.0, 1963.1, 2331.0, 2356.9, 2449.0, 3003.2, and 3514.7 keV. It has been checked that the number of cases of such energy coincidences is about what one should expect given the experimental resolution and the large number (~180) of γ rays between 0.3 and 4.3 MeV observed in this experiment.

An even more complicated case occurs for the 407G, which is well known as the only decay from 2773L. This level is strongly fed by 136G, 332G, and 436G. The 136G is too weak to be observed in this work, but is a known branch[36] from 2910L. After subtraction of these feedings, the excitation function is still monotonically increasing with a pronounced upward inflection at 3.4 MeV neutron energy [see Fig. 5(d)]. A careful search for other γ rays that could feed this level and account for the inflection was unsuccessful. Therefore, a second 407G deexciting 3453L is inferred. The resulting net excitation function for the first 407G from 2773L is smooth, but still monotonically increasing. This increase is consistent with the previous assignment of $J^\pi = 6^-$ for 2773L.

Thresholds of known γ decays (except for 1294G and 463G) were observed for all previously confirmed (observed in two or more experiments) levels below 3.1 MeV.[36] Six new levels between 2.9 and 3.2 MeV at 2996.3, 3016.6, 3105.4, 3157.9, 3179.7, and 3194.3 keV are proposed in this work. (All of these except 3017L were reported in Ref. 51.) The excitation functions leading to these new levels (except 3180L) are shown in Fig. 6. They are typical examples of how the many other new levels presented in this paper up to 4.3 MeV excitation

TABLE V. Summary of experimental results.

Other works[a]		This work			Thermal neutron capture		
E(level)[b] (keV)	$J^{\pi c}$	E(level)[b] (keV)	J^{π}	Preferred J^{π}	Intensity out(b)	Intensity in(b)	Intensity net(b)
0.0	0^+	0.0	0^+	0^+		43	
1293.54 *2*	2^+	1293.60[d] *3*	2^+	2^+	30	28	2
1756.78 *5*	0^+	1756.85[d] *3*	0^+	0^+	2.8	2.3	0.5
2027.3 *4*	0^+	2027.50 *4*	0^+	0^+	2.1	1.7	0.4
2112.26 *6*	2^+	2112.33 *3*	2^+	2^+	6.6	3.0	3.6
2225.35 *5*	2^+	2225.45 *3*	2^+	2^+	3.6	2.3	1.3
2266.09 *2*	3^-	2266.23 *3*	3^-	3^-	3.4	2.1	1.3
2365.92 *5*	5^-	2366.11 *8*	5^-	5^-	0.35	0.28	0.07
2390.8 *6*	4^+	2390.92 *3*	4^+	4^+	0.87	0.59	0.28
2529.12 *6*	4^+	2529.25 *4*	4^+	4^+	0.43	0.20	0.23
2546.0 *5*	$(0)^+$	2545.74 *3*	$(0)^+$	0^+	0.71	0.36	0.34
2586.7 *4*	(1^+)	2585.61 *3*	1^+	1^+	2.0	1.0	1.0
2650.5 *3*	2^+	2650.47 *3*	2^+	2^+	1.8	0.7	1.1
2773.25 *10*	6^-	2773.55 *13*	6^-	6^-	0.027	0.011	0.016
2790.6 *5*	$(2)^{+e}$	2790.57 *4*	$(0)^{+e}$	0^+	0.35	0.34	0.01
2801.7 *4*	4^+	2801.35 *5*	4^+	4^+	0.25	0.15	0.10
2843.5 *5*	2^+	2843.84 *5*	2^+	2^+	0.98	0.55	0.43
2908.8 *1*	7^-	2909.6[d] *5*	7^-	7^-			
2960.1 *3*	(2^+)	2960.07 *4*	2^+	2^+	0.83	0.61	0.22
2997 *3*	3^+	2996.29 *4*	3^+	3^+	0.52		0.52
		3016.58 *12*	$6^{(-)}$	6^-	0.047		0.047
3033.2 *5*	6^+	3032.2 *4*	6^+	6^+			
3046.51 *23*	4^+	3046.41 *10*	4^+	4^+	0.123		0.123
3088.6 *5*	(2^+)	3088.63 *5*	2^+	2^+	0.58	0.38	0.20
3096.63 *18*	(4^+)	3097.28 *23*	4^+	4^+		0.10	−0.10
3105.6 *5*	(7^-)	3105.35 *18*	5^-	5^-	0.029		0.029
		3157.87 *10*	3^-,4	4^-	0.104		0.104
3180 *3*	3^+	3179.72 *6*	2^+,3	3^+	0.32	0.09	0.23
		3194.34 *6*	0^+,1,3	0^+	0.44		0.44
3209.9 *5*	7^-	3210.1 *5*	7^-	7^-			
3227.9 *5*	8^-			8^-			
		3227.47 *5*	(2^+)	2^+	0.50	0.38	0.12
3228 *3*	$1^+,2^+,3^+$	3228.10 *15*	2^+	2^+	0.51		0.51
		3236.04 *6*	0^+,1,3	0^+	0.25	0.04	0.21
		3257.81 *14*	3^-,4,5^-	5^-	0.043		0.043
3276.7 *5*	(6^+)	3277.3[d] *6*	6^+	6^+			
		3289.06 *18*	<5	4^+	0.035		0.035
		3309.2 *4*	6^-	6^-			
3315 *3*	$3^+,4^+$	3315.04 *13*	$2^+,3^+$	3^+	0.41	0.03	0.38
3334.2 *10*	$1,2^+$	3333.81 *6*	1	1^-	1.21	0.34	0.87
		3344.39 *5*	2	2^+	0.54	0.59	−0.05
		3350.6 *4*	(5^+)	5^+			
3371 *3*	$1^+,2^+,3^+$	3371.44 *8*	3^+	3^+	0.178	0.044	0.134
3416 *3*	3^+	3415.9[f] *7*	$2,3^+$	3^+	0.15		0.15
		3416.58 *6*	2	2^-	0.30	0.10	0.20
		3427.98 *14*	4^-	4^-	0.09		0.09
3453.0 *3*		3453.9 *4*	4,5	4^-			
3470 *3*	$1^+,2^+,3^+$	3469.71 *9*	2^+	2^+	0.27	0.11	0.16
3492.9 *5*	8^+			8^+			
		3507.31 *21*	$3,4^-,5^-$	5^-	0.06		0.06
		3508.36 *7*	2^+	2^+	0.18	0.12	0.06
3513 *3*	$1^+,2^+,3^+$	3513.6 *3*	(2^+)	2^+	0.52	0.01	0.51
3522.5 *5*	9^-			9^-			
3547.0 *5*	10^+			10^+			
		3551.7 *5*	$2^+,3^+,4^+$	3^+	0.05		0.05
		3572.89 *11*	2^+,3	2^+	0.14		0.14
		3576.2 *6*	4^+,5	5^-			
3589 *3*	$1^+,2^+,3^+$	3586.63 *10*	2^+	2^+	0.28	0.05	0.23

TABLE V. (*Continued*).

Other works[a]		This work			Thermal neutron capture		
E(level)[b] (keV)	$J^{\pi c}$	E(level)[b] (keV)	J^{π}	Preferred J^{π}	Intensity out(b)	Intensity in(b)	Intensity net(b)
		3593.84 *9*	3^+	3^+	0.14	0.05	0.08
3618 *3*	$(1^+,2^+,3^+)$	3616.3 *4*	$2,3^-,4$	4^-			
		3624.6 *7*	$3^+,4^+$	4^+			
		3640.7 *7*	$4,5^+$	4^+			
		3648.1 *5*	$3^-,5^-$	5^-			
3658.1 *3*	$1,2^+$	3658.69 *6*	2^+	2^+	0.49	0.54	−0.05
3709 *3*	3^+	3706.9[g] *7*	$2^+,3^+,4^+$	3^+			
		3711.91 *7*	(1)	1^+	0.35	0.07	0.28
3713.9 *5*	8^+			8^+			
		3730.6 *4*	<4	0^+	0.10		
3739[h] *3*	(3^+)			3^+			
		3742.96 *18*	$1^-,2^+,3^-$	3^-	0.18		0.18
		3747.9 *4*	<4	0^+	0.07		0.07
3772 *3*	$1^+,2^+,3^+$	3776.79 *15*	1	1^+	0.16	0.04	0.12
		3787.3 *5*	(6^-)	6^-			
3797 *3*	$4^+,5^+$			4^+			
		3805.5 *6*	<5	4^+			
		3806.00 *17*	2^+	2^+	0.12	0.03	0.09
		3809.3 *8*	$2^+,3$	3^+			
		3836.69 *23*	<4	0^+	0.10		0.10
		3843.69 *19*	$2^+,3$	3^-	0.17		0.17
		3851.0 *5*	$1,2^+$	2^+	0.06		0.06
3887 *2*	(5^+)			5^+			
		3903.62 *22*	2^+	2^+	0.15	0.05	0.10
		3904.91 *6*	1	1^+	0.48	0.09	0.39
		3916.97 *6*	2	2^+	0.19	0.11	0.08
		3945.8 *5*	$1^+,2^+,3$	1^+	0.16		0.16
		3950.3 *3*	$1^-,2,3$	3^+	0.055		0.055
3950 *3*	$1^+,2^+,3^+$	3952.9 *3*	2^+	2^+	0.076	0.036	0.040
		3973.7 *8*	<5	4^+			
		4001.07 *6*	$1^{(-)}$	1^-	0.42	0.34	0.08
		4013.16 *11*	2^+	2^+	0.49	0.23	0.26
		4015.1 *6*	$2,3,4^+$	4^+			
4023 *2*	(5^+)			5^+			
		4026.75 *22*	1	1^+	0.13	0.06	0.07
		4028.5 *5*	<4	0^+	0.07		0.07
4037 *3*	$1^+,2^+,3^+$	4037.4 *3*	$2^+,3^+$	3^+	0.14	0.03	0.11
4076 *2*	$(4^+,5^+)$			4^+			
4084 *3*	$1^+,2^+,3^+$	4076.03 *20*	$1^+,2^+,3$	1^+	0.14	0.02	0.12
		4113.90 *6*	$1,2^+$	1^+	0.44	0.40	0.04
		4128.28 *20*	$1,2^+$	2^+	0.26		0.26
		4143.9 *5*	$1^+,2^+,3$	3^+	0.10		0.10
		4162.41 *11*	2	2^-	0.30	0.07	0.23
		4170.9 *4*	2^+	2^+	0.16		0.16
		4190.5 *4*	$2^+,3^+,4^+$	3^+	0.12		0.12
		4200.10 *14*	1	1^+	0.18		0.18
		4201.53 *6*	1,2	2^+	0.60	0.72	−0.12
		4211.59 *11*	$0^+,1,2$	2^+	0.22	0.06	0.16
		4238.50 *13*	2^+	2^+	0.12	0.15	−0.03
		4251.73 *10*	1	1^+	0.18	0.09	0.09
		4278.38 *17*	$1,2^+$	2^+	0.22	0.06	0.16
		4280.7 *7*	$2,3^-,4$	3^-			
4285 *3*	(7^+)			7^+			
		4297.1[i] *5*	<4	3^+	0.075		0.075
		. . .					
		. . .					

TABLE V. (*Continued*).

Other works[a]		This work			Thermal neutron capture		
E(level)[b] (keV)	$J^{\pi c}$	E(level)[b] (keV)	J^{π}	Preferred J^{π}	Intensity out(b)	Intensity in(b)	Intensity net(b)
4495.8 *5*	10^-			10^-			
4506.7 *10*	10^+			10^+			
4765 *2*	(7^+)			7^+			
4840 *2*	(10^-)			10^-			
4879.3 *5*	11^-			11^-			
5390.9 *8*	12^+			12^+			
		. . .					
		. . .					
		9563.56 *3*	$0^+,1^+$	$0^+,1^+$	8.1		

[a]Based on our evaluation of the existing literature (see Table I). The level energies and J^{π} values are generally consistent with those appearing in the Nuclear Data Sheets (1990).

[b]The notation is 1293.54 *2*≡1293.54±0.02, 1293.60 *3*≡1293.60±0.03, etc.

[c]For levels below 3.1 MeV and for the 3334.2- and 3658.1-keV levels, the J^{π} assignments are from the latest Nuclear Data Sheets (Ref. 36) unless noted otherwise. Above 3.1 MeV, they are from Refs. 11, 14, and 34.

[d]Level not supported by an $(n,n'\gamma)$ threshold.

[e]The 2^+ assignment for the 2790-keV level is from the angular distribution and cross section in the (d,p) reaction (Ref. 20). The intensities of the γ rays deexciting this level in the (n,γ) and $(n,n'\gamma)$ reactions, on the other hand, strongly favor a 0^+ assignment. See discussion in Sec. III D.

[f]Level created to agree with Ref. 34; otherwise could be combined with the 3416.58-keV level.

[g]Level created to agree with Ref. 34; not supported by an $(n,n'\gamma)$ threshold.

[h]The levels at this energy seen in the (d,t) and $(\alpha,t\gamma)$ reactions may not be the same.

[i]See Table III for levels above 4.3 MeV from the current work.

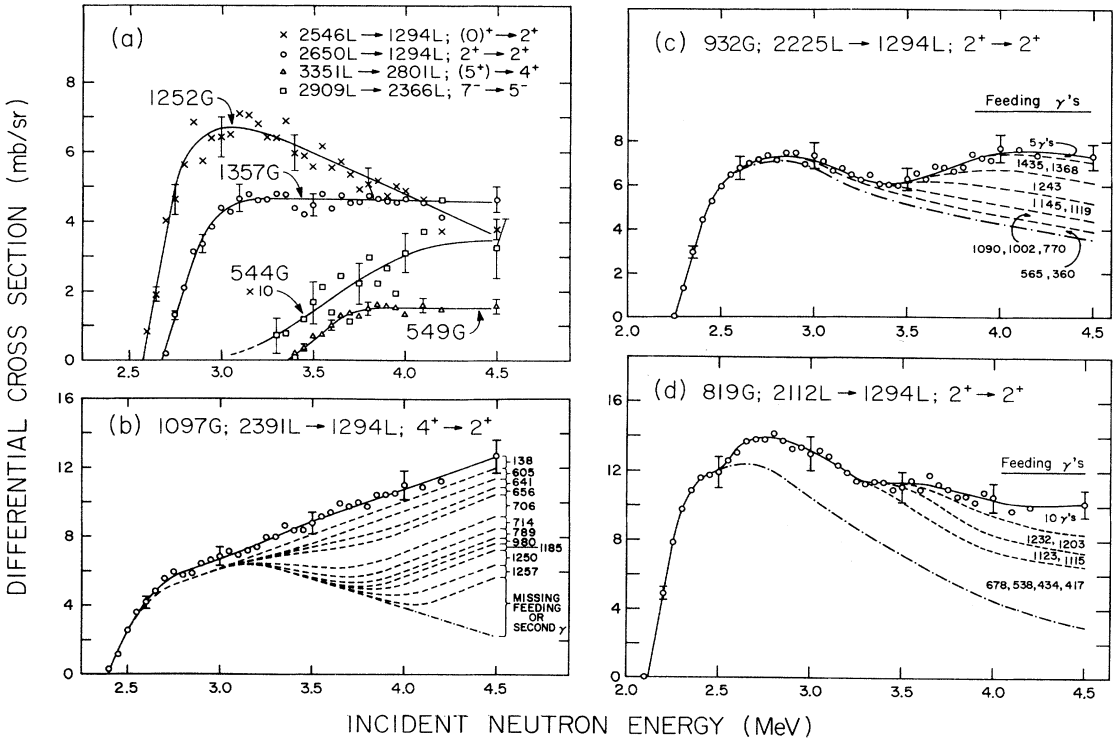

FIG. 4. Excitation functions of γ decays from levels in ^{116}Sn. (a) For the levels shown here that are populated mainly by inelastic neutron scattering, note how a higher spin value for the level correlates with a longer region of rising cross section above threshold. (b) The excitation function of 2391L is given by the data points and solid line. This level is fed by many γ decays from higher levels, with the feeding γ-ray energies tabulated on the right side. The excitation functions of the γ rays feeding 2391L are shown by the dashed lines, and they have been graphically subtracted to give the excitation function for direct excitation of the level as shown by the lowest dashed and dot-dashed lines. (c) The excitation function of 932G branch from 2225L. See above for a description of the dashed lines. The feeding γ-ray energies are listed between the dashed lines. (d) The excitation function of 819G branch from 2112L. See above for an explanation of the details of subtraction of the feeding.

were established. The 3105.4L found in this work is probably the same level as 3105.6L observed in the ^{114}Cd$(\alpha,2n\gamma)$ experiment of Bron *et al.*[12] Their measurements indicate $J^{\pi}=5^-$, 6^-, or 7^- for this level, consistent with the definite 5^- assignment of this work. Figure 6(c) shows the excitation function of 1901G which is the evidence for the new 3194L. This excitation function shows a second threshold which is interpreted as due to 1903G decay because no γ ray of $\sim$900 keV has a threshold near 4 MeV to cause such an effect. The 1903G fits as a decay from 4015L on the basis of both its intensity and angular distribution. The evidence (not shown here) for a second 417G is similar, and it is placed as a decay from 4076L.

C. Uncertain γ-ray placements

Some γ rays observed in this study could not be placed at all in the level scheme, and a smaller number could be placed, but not unambiguously. Those γ rays that were observed only in ^{115}Sn(n,γ) and have been left unplaced (approximately 25 out of 400 γ rays) either did not fit anywhere in the level scheme, or else had so many possible placements that it made little sense to choose one of them arbitrarily. Some γ rays seen in the ^{116}Sn$(n,n'\gamma)$ reaction were left unplaced because (a) they had no placement between pairs of established levels that was consistent with their threshold, (b) they had several possible placements consistent with the threshold, or (c) they had a placement consistent with the threshold, but the $(n,n'\gamma)$ branching ratio did not agree with the (n,γ) branching ratio. Only 9 out of 180 γ rays seen in the $(n,n'\gamma)$ experiment could not be placed, and all of them are very weak. For a few γ rays, there was enough information to severely limit the possible placements, but still there was some uncertainty. In general, these were cases where the γ-ray energy and the threshold energy were such that there was more than one possible final state for the decay, though often there was additional information available that led to a preferred placement. These cases are discussed in order of increasing γ-ray energy.

407.5 keV (II). The first 407G(I) is placed as

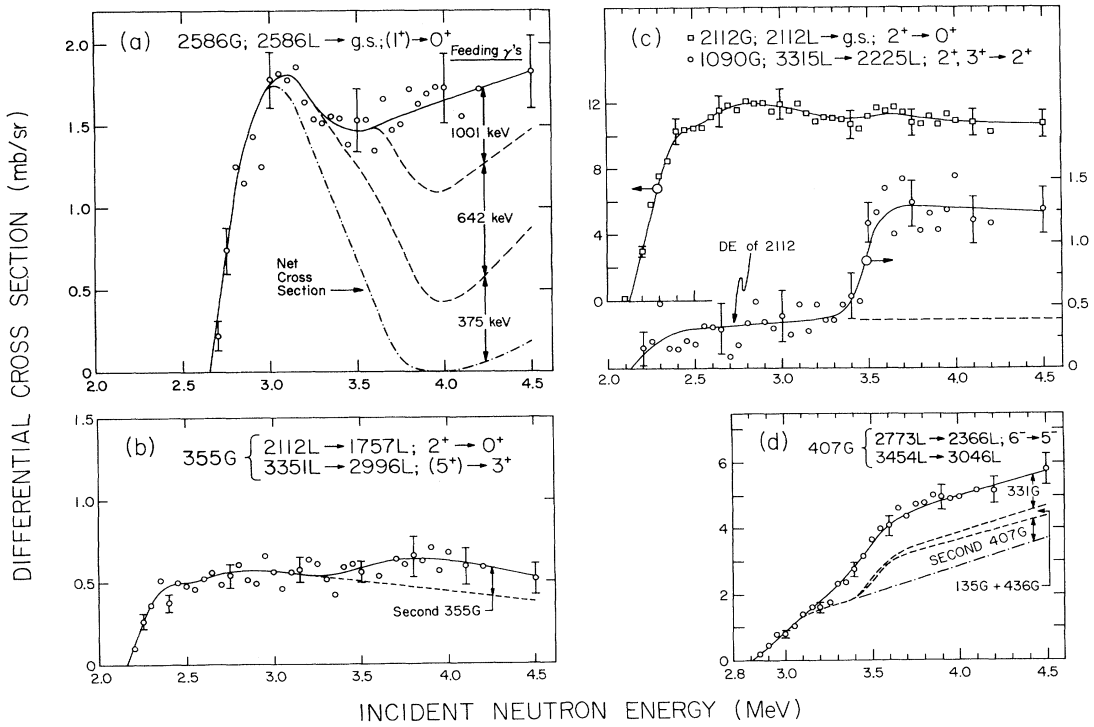

FIG. 5. Excitation functions of γ decays from levels in ^{116}Sn. (a) The excitation function of 2586L is given by the data points and solid line. Dashed lines show the graphical subtraction of the excitation cross section due to feeding. Because the net cross section from direct excitation by neutron scattering drops to zero, the existence of a γ-decay branch with an energy of 1292 keV is inferred. See text for further details. (b) The excitation function of 355G branch from 2112L. The rise in this excitation function at $E_n=3.4$ MeV is not seen in the excitation functions of the other γ decays [see Figs. 4(d) and 5(c)] from this level. From this observation, the existence of a second 355G with a threshold near 3.4 MeV is inferred. (c) Excitation functions of 2112G and 1090G. Below $E_n=3.3$ MeV, the cross section for 1090G is consistent with the measured double-escape (DE) detection efficiency for 2112G. Therefore, there is only one 1090-keV γ ray which comes from a level at about 3.3 MeV excitation. (d) Excitation function of two γ rays, both with an energy of 407 keV. The well-known 2774L has a single γ decay of 407.4 keV and is fed by 135G from 2909L, 332G from 3105L, and 436G from 3210L. The net excitation function shows a strong second threshold near $E_n=3.5$ MeV, implying the existence of a second 407-keV γ decay from a level near 3.5 MeV.

2774L→2366L. A strong second γ ray of this energy [407G(II)] is inferred from the second threshold seen at about 3.4 MeV after a careful subtraction of the feeding of 2774L by 436G, 331G, and 136G [see Fig. 5(d)]. The observed intensity of 407G in (n,γ) is quite weak, implying that these γ rays deexcite levels with $J \geq 5$; in fact, $J^{\pi}=6^{-}$ for 2774L. With this spin limit as a constraint, the only possible final states consistent with the threshold energy of 407G(II) are at 2910, 2996, 3017, 3032, 3046, 3097, and 3105 keV. Both the 2910L [see 543G in Fig. 4(a)] and 3017L can be eliminated because the feeding intensity would be two times stronger than the outgoing intensity. The excitation functions of the γ rays decaying from 2996L [see, for example, 1703G in Fig. 6(b)], 3032L, and 3097L show no sign of a rise at 3.4 MeV due to any 407G(II) feeding, thus eliminating these three levels. The γ decays from both 3046L and 3105L show some evidence of possible feeding in their excitation functions. On the basis of cross section systematics, there is some preference for assigning the decay as 3454L→3046L, but the other possibility (3512L→3105L) cannot be ruled out.

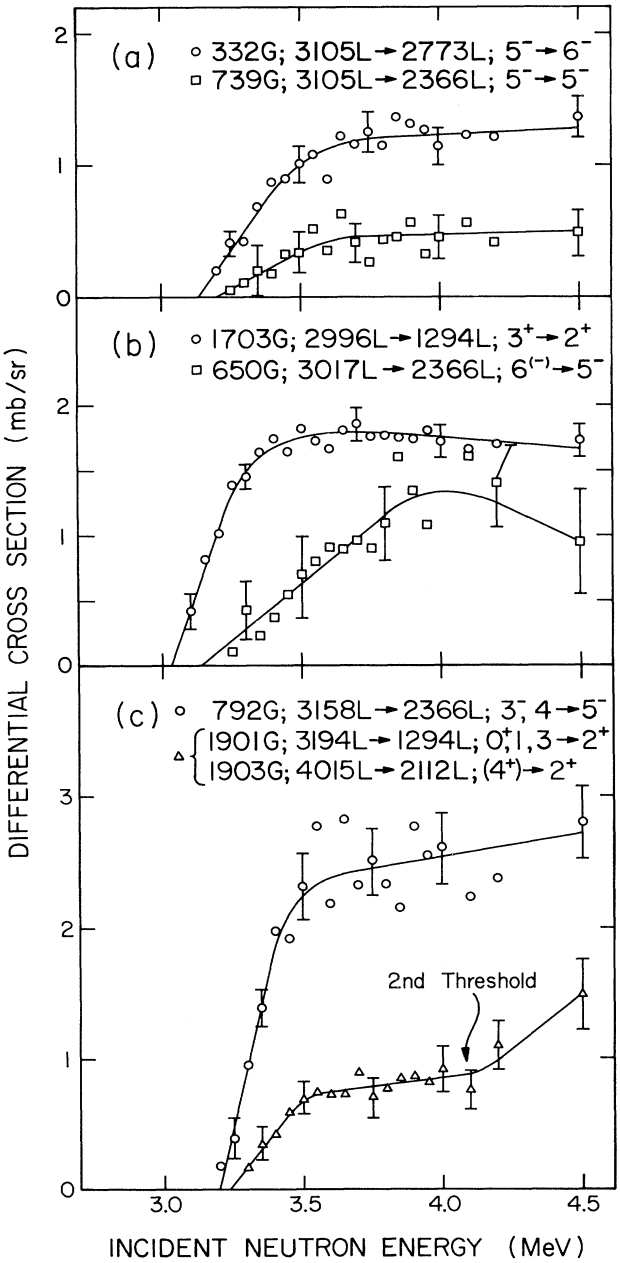

FIG. 6. Gamma-ray excitation functions that establish the existence of new levels. The second rise in the 1901G curve in (c) is interpreted as due to a second γ ray (1903G) because no strong γ ray was observed feeding the 3194L and accounting for this rise. The 1903G is placed as a decay from 4015L.

417.4 keV. The existence of this γ ray is inferred from a strong, sharp rise in the 417G excitation function (not shown) near $E_n=4.2$ MeV. The placement of this decay as 4076L→3659L is based on a good energy fit and agreement with predicted cross sections. It is also quite possible that this γ ray represents a decay from an unidentified state with no other strong γ rays.

678.28 keV. If the placement (2790L→2112L) of this γ ray is correct, the 678G/1497G branching ratio is such that this γ ray should have been observed in the γ spectrum of 14-sec ^{116}In β decay. However, 678G was not reported by Okano and Kawase[4] and the apparent upper limit for its intensity in their work is roughly half the expected intensity. Any other placement would require the creation of a new level.

891.69 keV. The energy of this γ ray agrees very well with the placement 3157L→2266L, but the threshold is noticeably different from that of 792G (3157L→2366L). Therefore, it is placed as 3257L→2366L. There is a small probability that the 3157L placement is the correct one.

1249.8 keV. Energetically, this γ ray could be placed as a decay from 3616L or 3640L. However, 1249G and 1350G cannot both decay from the same level because of differing excitation functions. The 1350G is placed as 3616L→2266L. Therefore, 1249G is placed as 3640L→2390L.

1350.1 keV. Although the excitation function of 1350G would allow the placement of 3576L→2225L, the threshold favors 3616L→2266L. Moreover, if 1350G were placed as a decay from the 3576L, the combined analysis of the angular distributions of 1350G and the 1185G out of this level would imply $J^{\pi}=2^{+},3$ for 3576L. Such a low-spin state should be readily observable in the (n,γ) reaction. Because neither 1185G nor 1350G were seen in the capture measurements, 1350G is placed as 3616L→2266L. With this placement, the angular distribution analyses now allow $J \geq 4$ for both 3576L and 3616L, accounting for the absence of the decays in (n,γ). This is a good example of the synergistic use of the (n,γ) and $(n,n'\gamma)$ measurements.

1421.1 keV. This is one of two cases where nonunique placements exist and where no other evidence was available to aid in determining a preferred placement. This γ ray is moderately strong in $(n,n'\gamma)$, but is not seen in (n,γ). The excitation-function threshold does not distinguish between the decays 3787L→2366L and 3812L→2390L, but does eliminate 3687L→2266L and

3950L→2529L. No other γ ray seen in $(n,n'\gamma)$ fits as a decay from 3787L or 3812L. Although there are at least five unplaced γ rays seen only in (n,γ) that could support either of these two levels on energy grounds, such placements must be rejected on intensity grounds. The 3787L→2366L placement was arbitrarily chosen for the 1421G, but the 3812L→2390L placement is equally possible.

1576.7 keV. This γ ray is placed as a decay from 4162L on the basis of its threshold and an excellent energy fit between otherwise established levels. There is some question about the placement, however, because it has little, if any, Doppler shift, while the other two decays of similar strength from the level show some shift. Any other possible placement as 4106L→2529L, 4122L→2545L, or 4227L→2650L would require the establishment of a new level based on a single decay.

1697.0 keV. This γ ray requires the introduction of a new level at 3809, 3963, 4063, or 4088 keV. The angular distribution and excitation function favor the 3809L→2112L placement with a $J^\pi=2^+$ or 3^+ assignment for 3809L.

1861.4 keV. Decays from 4086L, 3973L, or 3888L would be consistent with the observed threshold. Of these the 3973L→2112L placement is the preferred choice.

1963.7 keV. Based on the threshold information, 1964G could be placed as a decay from 4076L, 4188L, 4229L, or 4329L. From the observed cross section at $E_n=4.5$ MeV, the lowest energy placement 4076L→2112L is preferred, but the others cannot be ruled out.

2014.5 keV. The threshold information on this strong γ ray implies a level at 4126, 4240, 4280, 4380, or 4405 keV, with a preference for 4240L or 4280L. The choice of 4280L→2266L in Table II is arbitrary.

D. J^π assignments

Out of the 100 excited levels observed below 4.3 MeV excitation in the current work (see Table V), definite or tentative spin-parity assignments are given for 48 of them, and definite spin assignments (without parities) for another ten. For most of the others, the spin can be limited to a few values. These J^π assignments and limitations (also given in Table V) are based on the following types of information.

The low-lying levels of ^{116}Sn have been extensively studied in the past, resulting in well-established J^π assignments for many of them. Angular distributions together with the J^π of the final state give confident information about the J^π of the decaying level; the total intensity of the γ rays emitted by a level in the (n,γ) reaction provides supporting information. The $(n,n'\gamma)$ cross section for exciting a level is also dependent on the J^π and excitation energy of the level in a well-known way.[52–55] These cross sections also have a varying dependence on the incident neutron energy for different J^π values, so the shape of the excitation function can also be used as a secondary criterion for fixing J^π. Finally, the J^π limitations for allowed β decay, and l-transfer values from ^{117}Sn$(d,t)^{116}$Sn (Ref. 14), were used in a few cases to arrive at an assignment. The J^π assignments of levels up to 2366 keV were only tested for consistency with the $(n,n'\gamma)$ angular distributions. For all higher levels, a unique J^π assignment implies that other spin parities were excluded by application of the above criteria. The details will be presented in a paper currently in preparation, but the main results are given in Table V.

The current J^π assignments or limitations are consistent with those adopted in the Nuclear Data Sheets[36] with the exception of the assignment for 2790L. The $(2)^+$ assignment of Ref. 36 is based on the ^{115}Sn(d,p) studies of Schneid *et al.*[20] in which this level was observed to have $l_n=2$ and large spectroscopic strength, implying both $d_{3/2}\otimes s_{1/2}$ and $d_{5/2}\otimes s_{1/2}$, and, hence, $J^\pi=2^+$. The $(0)^+$ assignment of this work is based on the argument that the cross sections for populating this level in both the ^{115}Sn(n,γ) and ^{116}Sn$(n,n'\gamma)$ reactions agree very well with the observed systematics for populating 0^+ levels in this nucleus, but disagree strongly with those for the 1^+ and 2^+ levels. The current assignment was adopted in the further comparisons.

The values given under the "Preferred J^π" column in Table V are based on the following: (1) previous J^π assignments listed under the "Other work J^π" column, (2) present assignments under the "This work J^π" column, and (3) model considerations such as agreement with energy, decay properties, etc. The last-mentioned consideration, however, applies only to about a third of the preferred assignments.

E. Levels above 4.3 MeV

Above an excitation energy of 4.3 MeV, the proposed level scheme in this work (see Table III) is based on the (n,γ) data alone. Each level is defined by two or more transitions. In the absence of $(n,n'\gamma)$ threshold information, this part of the decay scheme is less certain than the part below 4.3 MeV. Alternate placements could not be excluded for several transitions. Multiple placements are a common problem in any reaction involving the observation of a large number of γ rays. They have been thoroughly checked in this work, and the placements presented here are the preferred ones based mainly on intensity considerations and the goodness of the energy fits.

F. Neutron separation energy

The neutron separation energy S_n determined in this work based on the old "mass-doublet standard" (Ref. 40) is 9563.56±0.03 keV. To convert to the "gold standard" the S_n value should be lowered by 94 eV. The uncertainty of 30 eV in the above S_n value arises from an overall least-squares fit applied to the entire decay scheme and does not include the uncertainty of the standards ($\sim$30 eV) or the uncertainty due to the above systematic correction (assumed to be half of 94 eV). Adding these uncertainties algebraically results in a final separation energy of $S_n=9563.47\pm0.11$ keV.

G. Thermal cross sections

The (n,γ) cross section based on the sum of the intensities of 45 secondary γ rays populating the ground state

is 43±5 b. This value is more precise than the currently adopted value[42] of 30±7 b. The total intensity of the ~67 discrete primary γ rays placed in the scheme (see Table III) is only ~8 b or ~20% of the cross section. This fraction is typical for medium-weight nuclei. In ^{116}Sn, the lowest 0^-, 1^-, and 2^- states are expected from theory to lie above 4.5 MeV (see Sec. IV). Therefore, most of the primary transitions observed in this work are $M1$ transitions.

IV. MODEL CALCULATIONS

Many previous experiments on ^{116}Sn have resulted in the observation of a particular subset of levels that has been interpreted in terms of one particular nuclear structure model. For instance, the observation of quasirotational bands in the even-A Sn isotopes by Fielding *et al.*[21] and by Bron *et al.*[12] led to the intruder-band calculations of Wenes *et al.*[59] Several such models are needed to describe various subsets of the excited levels of ^{116}Sn. An important question is whether the models proposed thus far are sufficient to account for the complete level scheme.

The nuclear models applied here to interpret the structure of ^{116}Sn include the shell model, a deformed collective model, and the collective vibrational model. Most of the observed levels can be identified with shell-model excitations involving only neutron orbitals and calculated with the two-broken-pair model of Bonsignori *et al.*[60] Shell-model excitations involving 1p-1h states are invoked phenomenologically and based largely on the results of particle-transfer reactions. The deformed collective model is needed to explain the intruder band of proton 2p-2h states and has also been used here to identify members of several other bands, while the multiphonon vibrational model works well to describe a number of states that have distinctive patterns of decay.

A. Two-broken-pair model

Because of the closed proton shell, the vast majority of low-lying levels in Sn isotopes will be neutron excitations. Due to the pairing property of the effective interaction between like nucleons, most of the valence neutrons (in the $50<N<82$ shell) will occur in Bardeen-Cooper-Schrieffer (BCS) pairs. It has already been demonstrated[60] that a good account of the energies as well as electromagnetic properties of the low-lying states in the even Sn nuclei may be given within such a model. It was shown that in truncating the complete valence shell-model space, it is important to employ configurations up to generalized seniority four [up to two broken pairs ($2bp$)]. In what follows, the calculation of Bonsignori *et al.*[60] is adopted as a starting point (see Table VI), which is then modified using phenomenological model concepts to produce a "best estimate" of the levels that may be expected in ^{116}Sn up to 4.3 MeV excitation energy.

In the calculation of Ref. 60, a Gaussian effective interaction between the neutrons was adopted, and the single-particle energies of the five valence shells $1g_{7/2}$, $2d_{5/2}$, $2d_{3/2}$, $3s_{1/2}$, and $1h_{11/2}$ were deduced from the levels of the adjacent odd Sn nuclei. The ground-state wave function was then found to consist mainly ($>95\%$) of a completely paired configuration (zero broken pairs)

$$|0bp\rangle = N_0 \left[\sum_j \alpha_j (a_j^\dagger a_j^\dagger)^{0^+} \right]^p |0\rangle \equiv N_0 (S^\dagger)^p |0\rangle \ , \tag{1}$$

where $p=8$ is the number of valence pairs in ^{116}Sn. Most of the low-lying states consist predominantly of configurations in which only one pair differs from those in the ground state, i.e., of one-broken-pair configurations

$$|1bp\rangle = \sum_{j'j''} C_{j'j''} (a_{j'}^\dagger a_{j''}^\dagger)^{J^\pi} (S^\dagger)^{p-1} |0\rangle \ . \tag{2}$$

It was also found, however, that such states, with the exception of the 2_1^+ state, generally contain considerable admixtures, of the order of 10–30%, of configurations with a second broken pair

$$|2bp\rangle = \sum_{1,2,3,4} C_{1,2,3,4} (a_1^\dagger a_2^\dagger a_3^\dagger a_4^\dagger)^{J^\pi} (S^\dagger)^{p-2} |0\rangle \ . \tag{3}$$

These admixtures of $2bp$ components are not only essential to explain certain electromagnetic properties but also cause a considerable downward shift in energy which can be as large as 300–500 keV.

With these considerations in mind, one may expect that the inclusion of configurations with three broken pairs into the model space will similarly yield considerable admixtures into the predominantly $2bp$ states and cause a downward shift of these states by half an MeV or so. An explicit calculation of this effect is not available because the formalism becomes quite complicated and the number of configurations very large. The size of this effect can be estimated by considering the data for the higher-spin states listed in Table VII. The energies of these states below 3.6 MeV, which are all predominantly $1bp$ states, are well reproduced (within 100 keV) by the calculation. The states above 4.3 MeV are $2bp$ states because there are no $1bp$ configurations with these J^π values with the exception of $J^\pi=10^+$. (For the 10^+ states above 4 MeV, the $1bp$ admixtures are so small that 100% $2bp$ is given in Table VI.) These $2bp$ states are calculated to be about 600 keV higher than found experimentally. It is assumed here that (1) this discrepancy is due to the omission of $3bp$ configurations in the model space and (2) all $2bp$ configurations would be pushed down by the same amount due to mixing with $3bp$ configurations. The recipe which has been applied to "correct" the calculated levels for this effect is expressed by

$$\begin{aligned} E_{J^\pi}(\text{corrected}) = E_{J^\pi}(\text{calculated}) \\ -[\,\%2bp \text{ in } \Psi(E_x) \\ -\%2bp \text{ in } \Psi_{\text{g.s.}}\,] \times 599 \text{ keV} \ . \end{aligned} \tag{4}$$

That is, the effect of adding a $3bp$ component to the $2bp$ calculation is assumed to be proportional to the amount of $2bp$ component in the wave function. After this admittedly primitive and rough "correction," *all* energies in Table VII agree with the data within 200 keV, which is typically as good an agreement as was found for states of

TABLE VI. Calculated energy levels (in keV) in ^{116}Sn together with their corresponding two-broken-pair admixtures (% 2*bp*) grouped according to their spin-parity (J^{π}) values.

No	*E*(level)	% 2*bp*	*E*(level)	% 2*bp*	*E*(level)	% 2*bp*	*E*(level)	% 2*pb*	*E*(level)	% 2*pb*	*E*(level)	% 2*bp*
	0^+ levels		0^- levels		1^+ levels		1^- levels		2^+ levels		2^- levels	
1	0	4	6361	100	2729	12	5220	100	1549	5	4680	26
2	1535	18	6710	100	3916	26	5493	100	2195	38	5058	96
3	2242	17	6780	100	3993	21	6179	100	2742	29	5323	97
4	2367	17	7184	100	4397	93	6231	100	2866	18	5401	92
5	3598	29	7517	100	4501	86	6334	100	3176	24	5593	99
6	3934	92	7669	100	4703	99	6499	100	3279	24	5669	96
7	4401	94			4785	99			3438	19		
8	4670	93			5075	98			3618	66		
9	5066	98			5246	99			4030	50		
10	5093	95			5276	99			4177	74		
	3^+ levels		3^- levels		4^+ levels		4^- levels		5^+ levels		5^- levels	
1	2920	21	3462	9	2501	23	2978	22	3272	15	2557	18
2	3190	29	3755	15	2977	28	3514	17	4287	20	3221	17
3	3264	19	4886	100	3071	19	3727	15	4407	95	3298	16
4	3697	17	5002	100	3247	21	4491	99	4742	98	3433	17
5	4218	86	5076	96	3642	67	4595	100	4851	98	4532	100
6	4311	25	5157	99	3957	38	4898	97	5134	100	4780	99
7	4580	97	5326	99	4379	49	5037	100	5199	100	4873	96
8	4646	95	5406	99	4515	73	5066	99	5306	100	4990	97
9	4748	87	5514	100	4572	68	5122	95	5420	100	5047	98
10	4796	98	5605	99	4637	97	5230	97	5468	100	5141	99
	6^+ levels		6^- levels		7^+ levels		7^- levels		8^+ levels		8^- levels	
1	3365	19	2734	21	5451	100	2835	18	3535	16	3127	19
2	3697	19	3182	20	5554	100	3134	20	5380	100	3938	18
3	4041	20	3364	17	5562	100	3410	17	5428	100	4796	97
4	4736	97	3584	18	5729	100	4495	99	5475	100	5036	98
5	5053	97	4621	93	6025	100	4885	98	5497	100	5082	99
6	5301	99	4695	95	6034	100	4975	97	5850	100	5164	99
7	5383	99	4892	100	6166	100	5013	99	6043	100	5223	99
8	5423	99	5035	99	6249	100	5102	98	6077	100	5300	100
9	5494	99	5094	96	6317	100	5174	100	6165	100	5483	95
10	5635	98	5124	97	6344	100	5180	99	6313	100	5601	100
	9^+ levels		9^- levels		10^+ levels		10^- levels		11^+ levels		11^- levels	
1	5433	100	3566	12	3443	19	5154	100	5549	100	5305	100
2	5573	100	5084	100	5500	100	5349	100	6259	100	6168	100
3	6276	100	5130	99	5559	100	5805	100	6442	100	6398	100
4	6341	100	5206	100	6128	100	6009	100	6467	100	6487	100
5	6390	100	5370	100	6230	100	6260	100	6570	100	6616	100

TABLE VI. (*Continued*).

No	E(level)	% 2bp	E(level)	% 2bp	E(level)	% 2bp	E(level)	% 2pb	E(level)	% 2pb	E(level)	% 2bp
	12^+ levels		12^- levels		13^+ levels		13^- levels		14^+ levels		14^- levels	
6			5392	94	6283	100	6314	100	6663	100	6696	100
7			5701	100	6432	100						
8			5783	100								
9			5853	100								
10			6118	100								
	15^+ levels		15^- levels		16^+ levels		16^- levels		17^- levels			
1	5989	100	6381	100	6430	100	6651	100	6601	100	7386	100
2	6503	100	6591	100	6542	100	7147	100	6712	100	7500	100
3	6515	100	6919	100	6731	100	7319	100	7022	100	7579	100
4	6716	100	7145	100	6833	100	7348	100	7073	100	7751	100
5	6830	100	7240	100	6995	100	7402	100	7219	100	8072	100
6	6860	100										
	16^+ levels		16^- levels		17^+ levels		17^- levels					
1	6952	100	7479	100	7435	100	7575	100	7658	100		
2	7319	100	7553	100	7695	100	8290	100				
3	7447	100	7759	100	8824	100						
4	8024	100	8137	100								

lower spin and lower energies.[60] The same correction, Eq. (4), was also applied to the lower-spin states.

B. Proton excitations

As indicated in Table VII, some of the excited states have been previously identified as proton excitations. The proton 2p-2h bands were first reported in $(\alpha,2n\gamma)$ reactions.[11–13] The $0^+(1757)$, $2^+(2112)$, $4^+(2529)$, $6^+(3032)$, $8^+(3714)$, and $10^+(4507)$ states in Table V belong to such an "intruder" band,[12] although the low-spin members are certainly mixed with neutron broken-pair excitations. In a semiphenomenological calculation, Wenes *et al.*[59] were able to reproduce such a band by coupling two proton particles to a ^{114}Cd core. The latter was constructed by first coupling two proton holes to a vibrational ^{116}Sn core, in the framework of a hole-phonon coupling model. Thus, the calculation includes the mixing of proton 2p-2h states that are built on top of quadrupole vibrations of ^{116}Sn, the largest components of which are neutron excitations of the open shells. Besides the observed intruder band, three other bands starting between 3 and 4 MeV were predicted by this calculation. It is expected that these proton 2p-2h states decay preferentially to states of the lowest proton 2p-2h band, since proton 1p-1h states are all higher in energy. It is this decay pattern that identifies a set of levels between 3 and 4 MeV which are compared in Sec. V A with the bands predicted by Wenes *et al.*[59] Support for the identification of the 3236-keV level (0^+) as the head of the second quasirotational band of Wenes *et al.*[59] (band "4" in Fig. 1 of Ref. 59) is found in the ^{114}Cd(^{3}He,n)^{116}Sn results of Fielding *et al.*[21] The latter group observed 0^+ levels at 1.84 and 3.42 MeV with very large proton pairing components.

Another class of proton excitations is the one-particle–one-hole states. In the ^{115}In(^{3}He,d) and ^{115}In(α,t) reactions,[14,17,34] states up to 3.7 MeV, apart from the 2_1^+ state, are very weakly excited. The 1p-1h excitations start at 3.7 MeV and extend to $\sim$4.5 MeV. Those with large spectroscopic factors start with a very strong state at 3887 keV, another one at 3950 keV, and several more between 4.0 and 4.3 MeV (see the "other works" column of Table V). The excitations at 3739, 3797, 4190, and 4238 keV are weaker, but this can be interpreted as resulting from the mixing of neutron components with the proton particle-hole components. Unfortunately, the spin values of all these states have not been definitely established, but they must arise from a coupling of the $g_{9/2}$ proton hole in In with a $d_{5/2}$ or $g_{7/2}$ proton particle corresponding to the lowest states in odd Sb. In comparing numbers of calculated and observed levels it is therefore assumed that a 2^+–7^+ multiplet of $(g_{9/2}^{-1},d_{5/2})$ type occurs around 4 MeV and a 1^+–8^+ multiplet of $(g_{9/2}^{-1},g_{7/2})$ a few hundred keV higher. In the comparison with calculated levels, those states at 3739, 3797, 3887, 3953, 4023, 4076, 4076.0, 4190, 4238, and 4285 keV (see Table V) excited strongly in the ^{115}In(^{3}He,d) and ^{115}In(α,t) reactions were assumed to be of this proton 1p-1h nature. This identification gives candidates for most of the low-spin members of these two multiplets.

TABLE VII. Possible correspondence between experimental and calculated levels with $J \geq 7$.

Experiment E_e(level) (keV)	J^π	J^π	Calculation E(level)[a] (keV)	% 2bp	E_c(level)[b] (keV)	Difference $(E_e - E_c)$ (keV)	Comments
2909.6 *5*	7^-	7^-	2835	18	2751	+159	
3210.1 *5*	7^-	7^-	3134	20	3038	+172	
3227.9 *5*	8^-	8^-	3127	19	3037	+191	
3492.9 *5*	8^+	8^+	3535	16	3463	+29	
3522.5 *5*	9^-	9^-	3566	12	3518	+5	
3547.0 *5*	10^+	10^+	3443	19	3353	+194	
3713.9 *5*	8^+	8^+					Proton 2p-2h band
4285 *3*	(7^+)	7^+					Proton 1p-1h
4495.8 *5*	10^-	10^-	5154	100	4578	−82	
4506.7 *10*	10^+	10^+					Proton 2p-2h band
4765 *2*	(7^+)	7^+	5451	100	4875	−110	
4840 *2*	(10^-)	10^-	5349	100	4773	+67	
4879.3 *5*	11^-	11^-	5305	100	4729	+150	
5390.9 *8*	12^+	12^+	5989	100	5413	−22	

[a]Calculated values listed in Table VI.
[b]Corrected values obtained with the use of Eq. (4).

C. Two-phonon states

In the calculations of Ref. 60, proton 1p-1h admixtures of the low-lying states were also calculated, especially for the collective 2_1^+ and 3_1^- states. It was found that these admixtures are only about 5% for the 2_1^+ state and that the energy of this state is reasonably well reproduced without such admixtures. For the 3_1^- state the situation is quite different. It consists almost equally of proton and neutron contributions. In a calculation with only valence neutrons, the energy of the 3_1^- state is more than 1 MeV too high, and a space of many proton as well as neutron shells is required to bring it down to the experimental energy. Because a calculation for two-phonon states involving octupole phonons within such a large model space would exceed tractable limits, these states are included in a phenomenological way, that is by simply adding up the experimental one-phonon energies and then looking in the experimental data for states with approximately the expected energies and the correct decay patterns.

Since the one-phonon 2_1^+ state is well described without any proton configurations, the 0^+, 2^+, and 4^+ triplet of two quadrupole phonons should be quite well reproduced by the *2bp* calculations. Therefore, the lowest states outside the neutron configuration space to be included phenomenologically are the $1^- - 5^-$ states composed of one quadrupole and one octupole phonon. Adding up the experimental energies one obtains 3.56 MeV as an estimate for their energy. Looking into the list of observed levels (see Table V), one finds possible candidates at 3334(1^-), 3417(2^-), 3428(4^-), 3507(5^-), and 3743(3^-) keV. For all but the 3334-keV level, this interpretation finds some support in their decay to the 3_1^- state. (Direct decay to the ground state is the energetically preferred mode for the decay of the 3334-keV level.) There are almost no other candidates for this two-phonon quintuplet among the observed levels.

States composed of two octupole phonons are expected around 4.5 MeV, which is at the upper border of the excitation energy region discussed here. Therefore, no attempt was made to find them, but the 0^+, 2^+, 4^+, and 6^+ states of this nature may appear just below 4.3 MeV.

D. Multiphonon states

Since three times the excitation energy of the 2_1^+ state is only 3.88 MeV, it is reasonable to expect some three-quadrupole-phonon states among the observed levels. The energies of these states as well as those of some four-phonon states up to 4.5 MeV can be estimated using either the SU(5) symmetry of the truncated quadrupole phonon model,[61] or its equivalent, the interacting boson model (IBM).[62] According to Ref. 62, the multiphonon states can be classified by the number of quadrupole phonons N; the boson seniority v (the number of phonons not pairwise coupled to zero angular momentum); a quantum number n_Δ, which is the number of triples of phonons coupled to zero angular momentum; and finally, the total angular momentum L. Within the present context, a quadrupole phonon corresponds to the presence of a d boson in the IBM, and N is therefore equivalent to n_d in Ref. 62. The excitation energies of the states were calculated using Eq. (4.21) of Ref. 62:

$$E(N,v,n_\Delta,L) = \hbar\omega_2 N + 0.5\alpha N(N-1) + \beta(N-v)(N+v+3) + \gamma[L(L+1)-6N] \ . \quad (5)$$

The parameters α, β, and γ are coefficients of two-boson interaction terms. Cubic terms in N that would arise from three-phonon interactions are neglected as usual in the IBM. The interaction energy C_L of two phonons coupled to angular momentum L is obtained by application of Eq. (5) for $N=2$. This yields the relationships [cf. Eq. (4.22) of Ref. 62]

$$C_0 = \alpha + 10\beta - 12\gamma, \ C_2 = \alpha - 6\gamma, \text{ and } C_4 = \alpha + 8\gamma \ . \quad (6)$$

The values $C_0 = -560$, $C_2 = -362$, and $C_4 = +214$ keV are obtained from the experimental two-phonon states at $2027(0^+)$, $2225(2^+)$, and $2801(4^+)$ keV. However, these states may be shifted due to mixing with other than multiphonon configurations. Moreover, the two-phonon strength is quite fragmented,[60] especially for the 4^+ state. (In particular, the two-phonon 4^+ can be thought of as distributed at least between 2390L and 2801L, and perhaps other nearby 4^+ levels.) It was therefore preferable to use the results of a calculation of the C_L that has been performed with the same broken-pair model as used for the other broken-pair states. In these microscopic IBM calculations,[63] the C_L values turned out to be rather dependent on the recipe used to construct the two-phonon states. Taking a reasonable average over the various results, acceptable values (in keV) are

$$-500 \leq C_0 \leq -350, \quad -250 \leq C_2 \leq -200 ,$$
$$\text{and } +100 \leq C_4 \leq +150 . \tag{7}$$

Using Eq. (6), the following parameters of Eq. (5) are deduced:

$$\alpha \approx -80 \text{ keV}; \ \beta \approx -5 \text{ keV}; \text{ and } \gamma \approx +25 \text{ keV} . \tag{8}$$

For large phonon numbers, the energies become sensitive to small changes in these parameters. In the spirit of the IBM, states up to $N = 8$ could occur where N is now the number of valence fermion pairs. Uncertainties in α, β, and γ and the neglect of possible contributions from three-phonon interactions, however, make predictions for such multiphonon-state energies less reliable with increasing N.

The list of multiphonon states with energies up to 4.5 MeV calculated with the parameters of Eq. (8) is given in Table VIII. Possible experimental candidates are also indicated there. They were selected on the basis of their preferential decay to the two-phonon or three-phonon states and/or close correspondence between calculated and experimental energies. The three-phonon states at $3228(2^+)$, $3371(3^+)$, and $3641(4^+)$ keV show the required preferential decay to the two-phonon states, and the 0^+ state at 3194 keV may also. The 2^+ state at 3228 keV may be strongly mixed with the normal two-broken-pair state identified with the experimental level at 3344 keV. The latter was selected on the basis of the observed decay of some of the supposed four-phonon states. Because of its dominant decay to the two-phonon 2^+ state at 2225 keV, it is also assumed that 2790L is strongly mixed with 3194L, sharing its three-phonon character. The four-phonon states at $4212(2^+)$ and $4480(4^+)$ keV are observed to have dominant decays to the three-phonon states identified above, making a rather convincing overall picture of multiphonon structure that is perhaps unexpected considering the possible mixing with other close-lying configurations of the same spin and parity.

TABLE VIII. Multiphonon states from microscopic IBM [see Eqs. (5) and (8)].

N	v	n_Δ	L	$E_{\text{calc.}}$	$E_{\text{expt.}}$
2	0	0	0	2157	2028
	2	0	2	2357	2225
	2	0	4	2707	2801 and 2390
3	3	1	0	3191	3194 and 2790
	1	0	2	3271	3228 and 3344
	3	0	3	3491	3371
	3	0	4	3691	3641
	3	0	6	4241	
4	0	0	0	3954	3837
	2	0	2	4154	4013
	4	1	2	4244	4212
	2	0	4	4504	4480
	4	0	4	4594	

V. COMPARISON OF THEORY AND EXPERIMENT

A. Possible correspondence between energy levels

For ease of comparison, it is convenient to group levels into three categories of high spin $J \geq 7$, intermediate spin $4 \leq J \leq 6$, and low spin $J \leq 3$. The comparisons are shown in Tables VII, IX, and X, respectively. Each experimental level is matched with a calculated level from the broken-pair model calculation, the proton 2p-2h calculation, the microscopic IBM calculation, or with a level from the phenomenological considerations in the preceding section. For the broken-pair-model states the percentage of two-broken-pair structure is also listed. The remaining part of the wave function is of one-broken-pair nature (zero-broken-pair nature for the ground state). For most levels identified as having non-2*bp* character, the decay pattern suggests their particular type of configuration. It is not claimed in these comparisons that the observed levels rigorously correspond to the theoretical counterparts shown here, since above 3 MeV there are many levels for which a unique spin and parity assignment is not available. Rather these tables are presented to illustrate that the overall numbers of theoretical and observed levels up to 4.3 MeV do agree and that such an attempt to bring theory and experiment into agreement exhibits no major discrepancies.

Two of the levels listed in Table X need some further explanation. The 3194-keV level, which is assumed to be a 0^+ state, is matched with the calculated 2*bp* state at 3406 keV, but its energy also agrees with that of the calculated three-phonon 0^+ state at 3191 keV (see Table VIII). This raises the question whether a three-phonon 0^+ state may be built of configurations with only two broken pairs. In microscopic calculations of two-phonon states,[63,64] it was found that the 0^+ states, in particular, are composed largely of configurations with fewer broken pairs than the corresponding number of phonons. Therefore, in the absence of additional information, it is assumed that *this* three-phonon state is the same as the two-broken-pair state.

The other level to be mentioned is the spin 1 state at 4252 keV. It is interpreted as a neutron 1^+ excitation, similar to the 2586-keV 1^+ state, built on top of the proton 2p-2h 0^+ state at 1757 keV. Note that such states were not included in the calculation of Wenes *et al.*[59] If this interpretation is correct, it is the lowest-energy state

of this type with a noncollective ingredient.

In Tables IX and X, several states are labeled as multiphonon states. One may ask whether such complicated states are expected to be excited in the current experiments. One argument in favor of a positive response is that proton 2p-2h states are also observed in spite of their complicated nature. Another argument is that in previous low-energy neutron-scattering experiments, multistep excitations were found to be important.[65] Multistep excitations occur especially for states which are coupled by large matrix elements. Therefore, it is not unlikely that multiphonon (low-spin) states can be observed in scattering experiments with low-energy neutron beams.

The average difference between the calculated and experimental energies for $2bp$ states with $J \leq 3$ is only 173 keV (neglecting the 3_1^- state, which has a large discrepancy of more than one MeV due to the neglect of proton 1p-1h components). For the $2bp$ states with $4 \leq J \leq 6$, this average discrepancy is only 101 keV. A reason for the larger discrepancy for low-spin states is probably that the interaction matrix elements, which are calculated with a simple Gaussian force, are largest for low-J values. For $J^\pi = 0^+$, they are typically as large as a few MeV and can easily differ by as much as 0.5 MeV from those of other phenomenological interactions such as a surface delta force. Therefore, the predicted energies may sometimes be off by as much as 0.5 MeV, as seen for the 0_3^+, 0_4^+, and 0_5^+ states. The average discrepancy between experiment and $2bp$ theory in Table X is 311 keV for the proposed 0^+ states and only 108 keV for the proposed 1^+ states.

B. Number and density of $J \leq 3$ states

A comparison of the numbers of predicted and observed excited states with $J \leq 3$ is listed in the upper part of Table XI. The numbers of calculated levels need some explanation. Consider the 2^+ states up to 3.9 MeV. Twelve levels were obtained from explicit calculations ($2bp$ and microscopic IBM) and four from phenomenology. The latter are identified in Table X. The total number of predicted levels, 16, agrees well with the observed number of 18 levels. When the excitation energy is extended to 4.3 MeV, the predicted and observed numbers

TABLE IX. Possible correspondence between experimental and calculated levels with $4 \leq J \leq 6$.

Experiment E_e(level) (keV)	J^π	Calculation J^π	% $2bp$	E_c(level)[a] (keV)	Difference $(E_e - E_c)$ (keV)	Comments
2366.11 *8*	5^-	5^-	18	2473	−107	
2390.92 *3*	4^+	4^+	23	2387	+4	Also two phonon
2529.25 *5*	4^+	4^+				Proton 2p-2h band 1
2773.55 *13*	6^-	6^-	21	2632	+141	
2801.35 *5*	4^+	4^+	28	2834	−32	Also two phonon
3016.58 *12*	$6^{(-)}$	6^-	20	3086	−69	
3032.2 *4*	6^+	6^+				Proton 2p-2h band 1
3046.41 *10*	4^+	4^+	19	2981	+65	
3097.28 *23*	4^+	4^+	21	3145	−48	
3105.35 *18*	5^-	5^-	17	3143	−38	
3157.87 *10*	3^-,4	4^-	22	2870	+288	
3257.81 *14*	3^-,4,5^-	5^-	16	3226	+32	
3277.3 *6*	6^+	6^+	19	3275	+2	
3289.06 *18*	<5	4^+	67	3264	+25	
3309.2 *4*	6^-	6^-	17	3286	+23	
3350.6 *4*	(5^+)	5^+	15	3206	+145	
3427.98 *14*	4^-	4^-				$2_1^+ \otimes 3_1^-$
3453.9 *4*	4,5	4^-	17	3436	+18	
3507.31 *21*	3,4^-,5^-	5^-				$2_1^+ \otimes 3_1^-$
3576.2 *6*	4^+,5	5^-	17	3355	+222	
3616.3 *4*	2,3^-,4	4^-	15	3661	−45	
3624.6 *7*	3^+,4^+	4^+	38	3753	−129	
3640.7 *7*	4,5^+	4^+				Three phonon
3648.1 *5*	3^-,5^-	5^-	100	3957	−309	
3787.3 *5*	(6^-)	6^-	18	3500	+287	
3797 *3*	4^+,5^+	4^+				Proton 1p-1h
3805.5 *6*	<5	4^+				Proton 2p-2h band 2
3887 *2*	(5^+)	5^+				Proton 1p-1h
3973.7 *8*	<5	4^+				Proton 2p-2h band 3
4015.1 *6*	2,3,4^+	4^+				Proton 2p-2h band 4
4023 *2*	(5^+)	5^+				Proton 1p-1h
4076 *2*	$(4^+,5^+)$	4^+				Proton 1p-1h

[a]Corrected values obtained from the values listed in Table VI with the use of Eq. (4).

TABLE X. Possible correspondence between experimental and calculated levels with $J \leq 3$.

Experiment		Calculation			Difference	
E_e(level) (keV)	J^π	J^π	% $2bp$	E_c(level)[a] (keV)	($E_e - E_c$) (keV)	Comments
0.0	0^+	0^+	4	0	0	
1293.60 *3*	2^+	2^+	5	1543	−250	
1756.85 *3*	0^+	0^+				Proton 2p-2h band 1
2027.50 *4*	0^+	0^+	18	1451	+577	Also two phonon
2112.33 *3*	2^+	2^+				Proton 2p-2h band 1
2225.45 *3*	2^+	2^+	38	1991	+234	Also two phonon
2266.23 *3*	3^-	3^-	9	3432	−1166	40% proton 1p-1h
2545.74 *3*	$(0)^+$	0^+	17	2164	+382	
2585.61 *3*	1^+	1^+	12	2681	−95	
2650.47 *3*	2^+	2^+	29	2592	+59	
2790.57 *4*	$(0)^+$	0^+	17	2289	+502	Also three phonon
2843.84 *5*	2^+	2^+	18	2782	+62	
2960.07 *4*	2^+	2^+	24	3056	−96	
2996.29 *4*	3^+	3^+	21	2818	+178	
3088.63 *5*	2^+	2^+				Proton 2p-2h band 2
3179.72 *6*	$2^+,3$	3^+	29	3042	+138	
3194.34 *7*	$0^+,1,3$	0^+	92	3406	−212	Also three phonon
3227.47 *5*	(2^+)	2^+	24	3159	+68	
3228.10 *15*	2^+	2^+				Three phonon
3236.04 *6*	$0^+,1,3^+$	0^+				Proton 2p-2h band 4
3315.04 *13*	$2^+,3^+$	3^+				Proton 2p-2h band 2
3333.81 *6*	1	1^-				$2_1^+ \otimes 3_1^-$
3344.39 *5*	2	2^+	66	3246	+98	Also three phonon
3371.44 *8*	3^+	3^+				Three phonon
3415.9 *7*	$2,3^+$	3^+	19	3174	+242	
3416.58 *6*	2	2^-				$2_1^+ \otimes 3_1^-$
3469.71 *9*	2^+	2^+	19	3348	+122	
3508.36 *7*	2^+	2^+				Proton 2p-2h band 4
3513.6 *3*	(2^+)	2^+	50	3754	−241	
3551.7 *5*	$2^+,3^+,4^+$	3^+	17	3619	−67	
3572.89 *11*	$2^+,3$	2^+	74	3757	−184	
3586.63 *10*	2^+	2^+				Proton 2p-2h band 3
3593.84 *9*	3^+	3^+	86	3726	−132	
3658.69 *6*	2^+	2^+	71	3790	−131	
3706.9 *7*	$2^+,3^+,4^+$	3^+	97	4022	−315	
3711.91 *7*	(1)	1^+	26	3784	−72	
3730.6 *4*	<4	0^+	29	3448	+283	
3739 *3*	(3^+)	3^+				Proton 1p-1h
3742.96 *18*	$1^-,2^+,3^-$	3^-				$2_1^+ \otimes 3_1^-$
3747.9 *4*	<4	0^+	94	3862	−114	
3776.79 *15*	1	1^+	93	3864	−87	
3806.00 *17*	2^+	2^+	84	4034	−228	
3809.3 *8*	$2^+,3$	3^+				Proton 2p-2h band 3
3836.69 *23*	<4	0^+				Four phonon
3843.69 *19*	$2^+,3$	3^-	15	3689	+165	
3851.0 *5*	$1,2^+$	2^+	61	4039	−188	
3903.62 *22*	2^+	2^+	88	4143	−239	
3904.91 *6*	1	1^+	21	3891	+14	
3916.97 *6*	2	2^+	95	4169	−252	
3945.8 *5*	$1^+,2^+,3$	1^+	86	4009	−63	
3950.3 *3*	$1^-,2,3$	3^+	95	4102	−152	
3952.9 *3*	2^+	2^+				Proton 1p-1h
4001.07 *6*	$1^{(-)}$	1^-				$2_2^+ \otimes 3_1^-$
4013.16 *11*	2^+	2^+				Four phonon
4026.75 *22*	1	1^+	99	4134	−117	
4028.5 *5*	<4	0^+	93	4137	−108	
4037.4 *3*	$2^+,3^+$	3^+	25	4182	−145	
4076.03 *20*	$1^+,2^+,3$	1^+				Proton 1p-1h

TABLE X. (*Continued*).

Experiment E_e(level) (keV)	J^π	Calculation J^π	% 2*bp*	E_c(level)[a] (keV)	Difference ($E_e - E_c$) (keV)	Comments
4113.90 *6*	$1,2^+$	1^+	99	4216	−102	
4128.28 *20*	$1,2^+$	2^+	96	4260	−132	
4143.9 *5*	$1^+,2^+,3$	3^+	98	4230	−86	
4162.41 *11*	2	2^-				$2_2^+ \otimes 3_1^-$
4170.9 *4*	2^+	2^+	90	4345	−174	
4190.5 *4*	$2^+,3^+,4^+$	3^+				Proton 1p-1h
4200.10 *14*	1	1^+	98	4511	−311	
4201.53 *6*	1,2	2^+	89	4455	−253	
4211.59 *11*	$0^+,1,2$	2^+				Four phonon
4238.50 *13*	2^+	2^+				Proton 1p-1h
4251.73 *10*	1	1^+				$1_1^+ \otimes 0_2^+$
4278.38 *17*	$1,2^+$	2^+	96	4474	−196	
4280.7 *7*	$2,3^-,4$	3^-	100	4310	−29	
4297.1 *5*	<4	3^+	87	4248	+49	

[a]Corrected values obtained from the values listed in Table VI with the use of Eq. (4).

are 25 and 28, respectively. Table XI shows good agreement between theory and data for all J^π values within the limits of current uncertainties. The agreement is worst for the 2^+ case but could be easily remedied by small changes in the constant, 599 keV, in Eq. (4). It is therefore quite possible that all states below 4.3 MeV with $J \leq 3$ have been observed in the current experiments. Note that the agreement between numbers of calculated and observed levels is equally good up to 3.7, 3.9, 4.1, and 4.3 MeV. This agreement implies that the broken-pair model, supplemented with the other models mentioned in Sec. IV, is satisfactory for predicting level densities of low-spin states up to at least 4.3 MeV excitation energy in this nucleus. It is then reasonable to assume that it also gives a valid prediction of the density of intermediate-spin states given in the lower part of Table XI. An estimate of such level densities is sometimes required as input in the calculation of the probabilities for various reaction channels.

C. Number of states with $4 \leq J \leq 6$

In the lower part of Table XI the numbers of predicted and observed excited states are listed for the intermediate

TABLE XI. Numbers of predicted (calculated + phenomenological) and experimentally observed levels up to an excitation energy of E^*.

	$E^*=3.7$ MeV		$E^*=3.9$ MeV		$E^*=4.1$ MeV		$E^*=4.3$ MeV	
J^π	Calc.[a]+Phen.[b]	Expt.[c]	Calc.[a]+Phen.[b]	Expt.[c]	Calc.[a]+Phen.[b]	Expt.[c]	Calc.[a]+Phen.[b]	Expt.[c]
0^+	6+2=8	7	7+2=9	9	8+2=10	10	9+2=11	11
0^-	0+0=0	0	0+0=0	0	0+0=0	0	0+0=0	0
1^+	1+0=1	1	4+0=4	3	5+1=6	7	7+2=9	10
1^-	0+1=1	1	0+1=1	1	0+2=2	2	0+2=2	2
2^+	9+4=13	16	12+4=16	18	14+5=19	22	19+6=25	28
2^-	0+1=1	1	0+1=1	1	0+1=1	1	0+2=2	2
3^+	5+1=6	7	6+3=9	10	7+3=10	12	11+4=15	15
3^-	2+0=2	1	2+1=3	3	2+1=3	3	3+1=4	4
$J \leq 3$	23+9=32	34	31+12=43	45	36+15=51	57	49+19=68	72
4^+	6+1=7	8	7+3=10	10	8+6=14	13	12+6=18	>13
4^-	3+1=4	4	3+1=4	4	5+1=6	4	5+1=6	>4
5^+	1+0=1	1	2+1=3	2	2+2=4	3	5+4=9	>3
5^-	4+1=5	6	4+1=5	6	5+1=6	6	6+1=7	>6
6^+	2+1=3	2	2+1=3	2	3+1=4	2	5+3=8	>2
6^-	4+0=4	3	4+0=4	4	5+0=5	4	6+0=6	>4
$4 \leq J \leq 6$	20+4=24	24	22+7=29	28	28+11=39	32	39+15=54	>32

[a]States calculated using the 2*bp* (Sec. IV A) and multi-quadrupole-phonon (Sec. IV D) models. See also Tables IX and X.
[b]All other phenomenologically identified states (See Sec. IV B, Sec. IV C, Table IX, and Table X).
[c]The levels from all experiments are listed in Table V.

spin values. These numbers clearly indicate that up to 3.9 MeV virtually all levels with $4 \leq J \leq 6$ have been detected, whereas between 4.1 and 4.3 MeV, 19–24 more levels with these spins remain to be observed. This is not surprising since it is well known that high-spin levels are not populated strongly either in the $(n,n'\gamma)$ reaction on a low-spin target near threshold or in the (n,γ) reaction when the capturing state has low spin. It should, of course, be mentioned that the good agreement for each individual J^π value up to 3.9 MeV in Table XI is somewhat contrived due to the particular J^π choices that have been made in Table IX. Nevertheless, it is satisfying that such good agreement may be obtained in this way.

D. Is the level scheme complete?

A major goal of this work was to establish a complete level scheme for ^{116}Sn up to some excitation energy. Tables VII–X contain all the levels predicted up to 4 MeV by the models discussed in Sec. IV, with the exception of a few $J \geq 5$ states above 3.3 MeV from the proton 2p-2h calculation.[59] To a good approximation, these models are "orthogonal" to each other in that the levels they predict are not redundant. As was pointed out above, the proton 1p-1h and 2p-2h excitations are truly outside the scope of the $2bp$ calculation and have been included here because of independent evidence for their character from other experiments. Insofar as the multiphonon excitations arise from $3bp$ (and higher) components of the wave function or from proton excitations, they are also outside the scope of the $2bp$ calculation, and can be added without fear of double counting.

An experimental candidate with appropriate properties (J^π, energy, decay pattern, etc.) has been found for each of the predicted levels shown. If anything, Table XI shows a small *excess* of observed low-spin levels for $3.7 \leq E_x \leq 4.3$ MeV, but as discussed above for the 2^+ levels, this excess could be easily corrected by a slight increase in the $2bp$ energy correction parameter in Eq. (4). The situation is, therefore, that every experimental level has a realistic model identification, and an experimental candidate has been found for every model level below 4 MeV that should have been seen in these experiments. It would be extremely fortuitous for this to happen by accident, given the large number of levels and models involved. It is therefore concluded that with good probability the level scheme is complete or nearly complete up to 4.0 MeV excitation energy in ^{116}Sn.

VI. FLUCTUATION PROPERTIES

A topic of great interest today throughout all areas of physics is chaos. While chaos in classical systems is both well defined and well understood, the same cannot be said for quantum systems; there the search for a consistent and useful definition continues. One approach is to study the fluctuation properties of the energy levels of the quantum system; this dates back to the analysis of the fluctuation properties of the quantum Sinai's billiard by Bohigas, Giannoni, and Schmit.[66] They offered the conjecture that time-reversal-invariant systems whose classical analogs are chaotic show fluctuation properties described by the Gaussian orthogonal ensemble (GOE) of random matrix theory.[67] Since that time, analyses of a number of relatively simple mathematical systems[68–71] have shown GOE behavior for systems whose classical analogs are chaotic and Poisson behavior for systems whose classical analogs are integrable. While exceptions to this generalization are known,[72–74] the available evidence strongly suggests a connection between the quantum fluctuation properties and the underlying chaoticity or regularity of the system. Analysis of appropriate experimental data may thus offer new insights into the behavior of the experimental system.

Because missing or misassigned levels will severely affect the fluctuation properties, one of the requirements for a fluctuation analysis is data of the highest possible quality. The best available level scheme in this regard is probably that of ^{26}Al, where 160 levels are known in the region of excitation energy 0–8 MeV (Ref. 75). There the fluctuation properties showed behavior between GOE and Poisson.[3,76] The nearly complete level scheme for ^{116}Sn presented here makes this nuclide an additional excellent candidate for this type of analysis.

In this discussion, we shall concentrate on the probability distribution of spacings S_i between adjacent levels with the same symmetries (J and π in this case). It proves simplest to express the distribution in terms of the dimensionless parameter $x \equiv S/D$, where D is the average spacing. If the behavior is GOE, then the spacing distribution is very nearly a Wigner distribution:[77]

$$P(x) = \frac{\pi}{2} x e^{-\pi(x^2/4)} . \tag{9}$$

If the behavior is Poisson, then

$$P(x) = e^{-x} . \tag{10}$$

An interpolation formula between these two extremes has been proposed by Brody:[78]

$$P(x;\omega) = \alpha(\omega+1)x^{\omega} e^{-\alpha x^{\omega+1}} ;$$
$$\alpha = \left[\Gamma\left[\frac{\omega+2}{\omega+1} \right] \right]^{\omega+1} . \tag{11}$$

In this expression $\omega = 0$ corresponds to a Poisson distribution, and $\omega = 1$ to a GOE distribution; the distribution is nonlinear, and a distribution halfway between GOE and Poisson corresponds to $\omega \approx 0.4$. It should be emphasized that ω has no known physical significance, but it does provide a convenient method of characterizing the nearest-neighbor spacing (NNS) distributions.

The method of analysis has been described in detail in Ref. 76, and only an outline will be given here. Because random matrix theory only applies to a group of levels with the same quantum numbers, the data must be separated into such groups (which we shall label "sequences"). We require a sequence to have a minimum of five levels before including it in this analysis; therefore, only the 0^+, 1^+, 2^+, 3^+, 4^+, and 5^- sequences in ^{116}Sn have been included. In all cases, the preferred assignment shown in Table V has been used. The NNS distribution was determined for each of these sequences, and

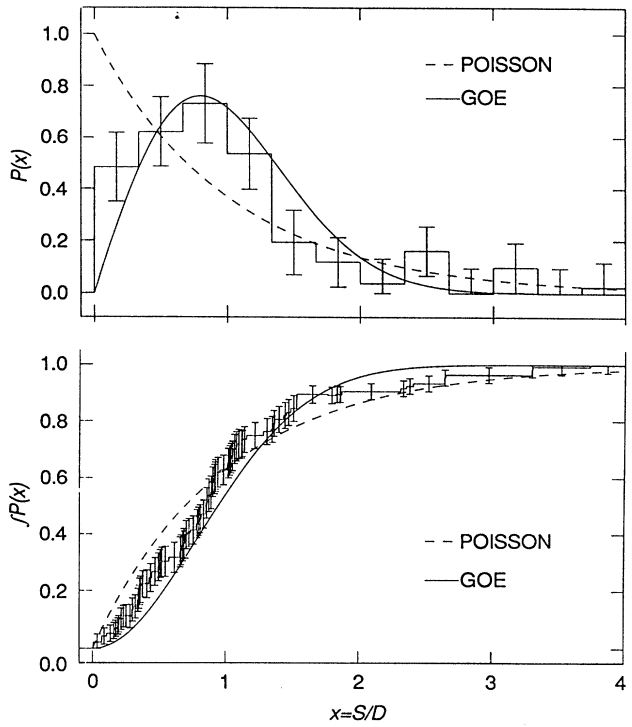

FIG. 7. The nearest-neighbor spacing distribution $P(x)$ and its integral for levels in ^{116}Sn. See Sec. VI for related discussion, especially Eqs. (9) and (10). The experimental distribution for 0^+, 1^+, 2^+, 3^+, 4^+, and 5^- levels lies between a Gaussian orthogonal ensemble (GOE) and Poisson distributions.

the results averaged to yield an overall NNS distribution $P(x)$ for ^{116}Sn, which is shown in Fig. 7 along with its integral. The experimental distribution generally lies between a GOE and a Poisson distribution, with a best fit of $\omega=0.51\pm0.19$. By comparison, a similar analysis carried out for the states (both positive and negative parity) in ^{26}Al yielded[76] $\omega=0.47\pm0.14$.

VII. SUMMARY

The bound states of ^{116}Sn and their decays have been studied using the ^{115}Sn(n,γ) and ^{116}Sn$(n,n'\gamma)$ reactions. Below an excitation energy of 4.3 MeV, 100 excited states have been identified, and unique spin assignments have been made for more than half of them. For most of the rest, the spin has been limited to no more than three possibilities. The experimental identification of these levels is reliable because it depends on consistency of the information from both reactions as well as with published results on this nucleus. The possible existence of 55 additional levels has been established between 4.3 and 7.7 MeV from the (n,γ) data alone. Based on the J^π values of the levels below 4.3 MeV excited in the (n,γ) reaction, these additional levels probably all have $J\leq4$. The neutron separation energy of ^{116}Sn was measured to be 9563.47±0.11 keV.

Five different types of excitation of the ^{116}Sn nucleus have been identified in this work on the basis of γ-decay patterns and agreement with predicted energies, spins, and parities. Candidates for all four bands of the proton 2p-2h intruder-band excitation calculated by Wenes *et al.*[59] have been proposed, whereas only the lowest-lying band had been previously identified. Many levels are seen that agree well with quadrupole three-phonon and four-phonon states calculated in an IBM description in the SU(5) limit. In a more phenomenological spirit, all levels of a quadrupole-octupole quintet, and most of the levels due to the proton $(g_{9/2}^{-1},d_{5/2})$ and $(g_{9/2}^{-1},g_{7/2})$ configurations, have been located, the latter with much help from previously published works. All remaining states, about 70% of the total, are found to agree well with the neutron shell *2bp* calculations of Bonsignori *et al.*[60] These five types of structures account for all but one of the observed levels; conversely, up to 4 MeV excitation energy almost no predicted level is missing, thus illustrating the nonselectivity and sensitivity of these neutron-induced reactions. The detailed comparisons presented in this paper indicate with good reliability that most, if not all, excited states with $J\leq3$ have been identified up to 4.3 MeV excitation, and similarly for levels with $4\leq J\leq6$ up to 3.9 MeV, and possibly even 4.0 MeV excitation. The verification of this claim as well as firmer spin and parity assignments for all levels must await future experiments.

From a theorist's point of view, there is at present no compelling evidence that requires the introduction of any new type of excitation because the existing models are sufficient to account for the levels up to 4 MeV in ^{116}Sn. However, it is recognized that for a definitive comparison, it would be necessary to do a more complete calculation, involving both neutron and proton configurations, to a higher order than hitherto attempted.

The nearest-neighbor spacing distribution for ^{116}Sn shows behavior intermediate between a Gaussian orthogonal ensemble description and a Poisson description. What this means is not well understood. It might indicate a region which is neither purely chaotic nor purely regular. Such behavior could also be seen if another good (or nearly good) quantum number is necessary to describe these states, even if the underlying behavior is GOE.[79] Further understanding of this aspect of nuclear behavior requires additional work on both the experimental and theoretical fronts.

ACKNOWLEDGMENTS

We acknowledge the help of Bill Starner in taking the ^{115}Sn(n,γ) data at Los Alamos and of John Hanly, Steve Hicks, Steve O'Brien, Shi Xiamin, Zhou Zuying, and Cao Zhong, in taking the ^{116}Sn$(n,n'\gamma)$ data at Lexington. R. F. Carlton participated in the early stages of the ^{115}Sn(n,γ) work. We thank M. J. Martin and M. T. McEllistrem for critical readings of the manuscript. Support for one of us (T.A.W.) was provided by the Oak Ridge Associated Universities, and a sabbatical leave was provided by Edinboro University of Pennsylvania. This work was sponsored in part by the U.S. Department of Energy under Contract No. DE-AC05-84OR21400 with Martin Marietta Energy Systems, Inc. (Oak Ridge); Con-

tract No. W-7405-Eng-35 with the University of California (Los Alamos); and Grant No. DE-FG05-87ER40353 with Tennessee Technological University and by the U.S. National Science Foundation under Grant No. PHY-8702369 with the University of Kentucky. It was sponsored in part also by the Netherlands Foundation for Fundamental Research on Matter (FOM), which is financially supported by the Netherlands Organization for Pure Scientific Research (ZWO).

---

*Permanent address: Edinboro University of Pennsylvania, Edinboro, Pennsylvania 16444.

†Permanent address: Nuclear Research Centre—Negev, Beer-Sheva, Israel.

‡Permanent address: Ministry of Light Industry, Fu-Cheng Men, Beijing, China.

§Permanent address: Institute of Nuclear Research (ATOMKI), Debrecen, Hungary.

[1]A. Y. Abul-Magd and H. A. Weidenmüller, Phys. Lett. **162B**, 223 (1985).

[2]T. von Egidy, A. N. Bekhami, and H. H. Schmidt, Nucl. Phys. **A454**, 109 (1986); T. von Egidy, H. H. Schmidt, and A. N. Bekhami, *ibid.* **A481**, 189 (1988).

[3]G. E. Mitchell, E. G. Bilpuch, P. M. Endt, and J. F. Shriner, Jr., Phys. Rev. Lett. **61**, 1473 (1988).

[4]K. Okano and Y. Kawase, Nucl. Instrum. Methods **108**, 503 (1973); and private communication.

[5]D. Rabenstein, Z. Phys. **240**, 244 (1970).

[6]G. Ardisson, Radiochem. Radioanal. Lett. **16**, 241 (1974).

[7]Y. Yamaguchi, J. Ruan(Gen), and T. Nagahara, J. Phys. Soc. Jpn. **38**, 911 (1975).

[8]R. J. Gehrke and L. D. McIsaac, Aerojet Nuclear Company Report ANCR-1088, 1972, p. 379.

[9]L. L. Riedinger, R. W. Lide, L. H. Harwood, and C. R. Bingham, Oak Ridge National Laboratory Report ORNL-4937, 1974, p. 62.

[10]T. Yamazaki and G. T. Ewan, Nucl. Phys. **A134**, 81 (1969).

[11]A. van Poelgeest, Ph.D. dissertation, Vrije Universiteit, Amsterdam, 1978.

[12]J. Bron, W. H. A. Hesselink, A. van Poelgeest, J. J. A. Zalmstra, M. J. Uitzinger, H. Verheul, K. Heyde, M. Waroquier, H. Vincx, and P. van Isacker, Nucl. Phys. **A318**, 335 (1979).

[13]A. van Poelgeest, J. Bron, W. H. A. Hesselink, K. Allaart, J. J. A. Zalmstra, M. J. Uitzinger, and H. Verheul, Nucl. Phys. **A346**, 70 (1980).

[14]J. M. Schippers, Ph.D. dissertation, Rijksuniversiteit, Groningen, 1988.

[15]J. A. Biggerstaff, C. Bingham, P. D. Miller, J. Solomon, and K. K. Seth, Phys. Lett. **25B**, 273 (1967).

[16]R. Shoup, J. D. Fox, and G. Vourvopoulos, Nucl. Phys. **A135**, 689 (1969).

[17]S. Y. van der Werf, N. Blasi, M. N. Harakeh, G. Wenes, A. D. Bacher, G. T. Emery, C. W. Glover, W. P. Jones, H. J. Karwowski, H. Nann, C. Olmer, P. den Heijer, C. W. de Jager, H. de Vries, J. Ryckebusch, and M. Waroquier, Phys. Lett. **166B**, 372 (1986).

[18]D. A. McClure and J. W. Lewis, III, Phys. Rev. C **5**, 922 (1972).

[19]E. A. Rudak, A. V. Soroka, and V. N. Tadzush, *Program and Theses, 28th Annual Conference on Nuclear Spectroscopy and Nuclear Structure of Atomic Nuclei, Alma-Ata, 1978* ("Nauka," Leningrad, 1978), p. 43; and private communication.

[20]E. J. Schneid, A. Prakash, and B. L. Cohen, Phys. Rev. **156**, 1316 (1967).

[21]H. W. Fielding, R. E. Anderson, C. D. Zafiratos, D. A. Lind, F. E. Cecil, H. H. Wieman, and W. P. Alford, Nucl. Phys. **A281**, 389 (1977).

[22]Phan Xuan Ho, J. Bellicard, P. Leconte, and I. Sick, Nucl. Phys. **A210**, 189 (1973).

[23]D. L. Allan, B. H. Armitage, and B. A. Doran, Nucl. Phys. **66**, 481 (1965).

[24]O. Beer, A. El Behay, P. Lopato, Y. Terrien, G. Vallois, and K. K. Seth, Nucl. Phys. **A147**, 326 (1970).

[25]H. Wienke, H. P. Blok, and J. Blok, Nucl. Phys. **A405**, 237 (1983).

[26]A. Bäcklin, W. Dietrich, R. Julin, J. Kantele, M. Luontama, and L. Westerberg, Phys. Lett. **62B**, 402 (1976).

[27]J. Kantele, R. Julin, M. Luontama, A. Passoja, T. Poikolainen, A. Bäcklin, and N.-G. Jonsson, Z. Phys. A **289**, 157 (1979).

[28]A. Bäcklin, N. G. Jonsson, R. Julin, J. Kantele, M. Luontama, A. Passoja, and T. Poikolainen, Nucl. Phys. **A351**, 490 (1981).

[29]N.-G. Jonsson, A. Bäcklin, J. Kantele, R. Julin, M. Luontama, and A. Passoja, Nucl. Phys. **A371**, 333 (1981).

[30]A. M. Demidov, L. I. Govor, Yu. K. Cherepantsev, M. R. Ahmed, S. Al-Najjar, M. A. Al-Amili, N. Al-Assafi, and N. Rammo, *Atlas of Gamma-Ray Spectra From the Inelastic Scattering of Reactor Fast Neutrons* (Moscow Atomizdat, Mosow, 1978), p. 172.

[31]Y. S. Kim and B. L. Cohen, Phys. Rev. **142**, 788 (1966).

[32]K. Yagi, Y. Saji, T. Ishimatsu, Y. Ishizaki, M. Matoba, Y. Nakajima, and C. Y. Huang, Nucl. Phys. **A111**, 129 (1968).

[33]D. G. Fleming, Can. J. Phys. **60**, 428 (1982).

[34]J. Schreuder, J. M. Schippers, and S. Y. van der Werf, Kernfysisch Versneller Instituut (KVI) annual report, 1987; J. M. Schippers, J. M. Schreuder, S. Y. van der Werf, K. Allaart, N. Blasi, and M. Waroquier, Nucl. Phys. **A510**, 70 (1990).

[35]D. G. Fleming, M. Blann, H. W. Fulbright, and J. A. Robbins, Nucl. Phys. **A157**, 1 (1970).

[36]G. H. Carlson, W. L. Talbert, Jr., and S. Raman, Nucl. Data Sheets **14**, 247 (1975); J. Blachot, J. P. Husson, J. Oms, G. Marguier, and F. Haas, *ibid.* **32**, 287 (1981); J. Blachot and G. Marguier, *ibid.* **59**, 333 (1990).

[37]S. Raman, R. F. Carlton, J. C. Wells, E. T. Jurney, and J. E. Lynn, Phys. Rev. C **32**, 18 (1985).

[38]W. K. Dagenhart, P. H. Stelson, F. K. McGowan, R. L. Robinson, W. T. Milner, S. Raman, and W. K. Tuttle, III, Nucl. Phys. **A284**, 484 (1977).

[39]S. Raman, in *Neutron Capture Gamma Ray Spectroscopy and Related Topics 1981,* edited by T. von Egidy, F. Gönnenwein, and B. Maier (Institute of Physics, Bristol, 1982), p. 357.

[40]S. Raman, E. T. Jurney, D. A. Outlaw, and I. S. Towner, Phys. Rev. C **27**, 1188 (1983).

[41]*Table of Isotopes,* Seventh edition, edited by C. M. Lederer and V. S. Shirley (Wiley, New York, 1978).

[42]S. F. Mughabghab and D. I. Garber, *Neutron Cross Sections, Volume I, Resonance Parameters,* Brookhaven National Laboratory Report BNL-325, 1973, p. 1-1.

[43]R. W. Harper, T. W. Godfrey, and J. L. Weil, Phys. Rev. C

26, 1432 (1982).
[44]J. D. Brandenberger, Nucl. Instrum. Methods **69**, 271 (1969).
[45]J. P. Fouan and J. P. Passerieux, Nucl. Instrum. Methods **62**, 327 (1968).
[46]G. P. Glasgow, F. D. McDaniel, J. L. Weil, J. D. Brandenberger, and M. T. McEllistrem, Phys. Rev. C **18**, 2520 (1978).
[47]M. T. McEllistrem, private communication.
[48]M. T. McEllistrem, in *Nuclear Research with Low Energy Accelerators,* edited by J. B. Marion and D. M. Van Patter (Academic, New York, 1967), p. 167.
[49]R. F. Carlton, S. Raman, and E. T. Jurney, in *Neutron Capture Gamma-Ray Spectroscopy,* edited by R. E. Chrien and W. R. Kane (Plenum, New York, 1979), p. 571.
[50]J. Sa, Z. Cao, J. Hanly, S. P. O'Brien, M. H. Yang, S. E. Hicks, and J. L. Weil, Bull. Am. Phys. Soc. **28**, 976 (1983).
[51]Z. Gácsi, J. Sa, J. L. Weil, E. T. Jurney, and S. Raman, in *Capture Gamma-Ray Spectroscopy and Related Topics-1984,* Proceedings of the Fifth International Symposium on Capture Gamma-Ray Spectroscopy and Related Topics, edited by S. Raman, AIP Conf. Proc. No. 125 (AIP, New York, 1985), p. 539; Bull. Am. Phys. Soc. **29**, 1041 (1984).
[52]L. Wolfenstein, Phys. Rev. **82**, 690 (1951).
[53]W. Hauser and H. Feshbach, Phys. Rev. **87**, 366 (1952).
[54]J. W. Tepel, H. M. Hofman, and H. A. Weidenmüller, Phys. Lett. **49B**, 1 (1974).
[55]J. W. Tepel, H. M. Hofman, and M. Herman, in *Proceedings International Conference on Nuclear Cross Sections for Technology,* edited by J. L. Fowler, C. H. Johnson, and C. D. Bowman, Natl. Bur. Stand. (U.S.) Spec. Publ. No. 594 (U.S. GPO, Washington, DC, 1980), p. 762.
[56]A. J. Filo, S. W. Yates, D. F. Coope, J. L. Weil, and M. T. McEllistrem, Phys. Rev. C **23**, 1938 (1981).
[57]B. D. Kern, M. T. McEllistrem, J. L. Weil, and S. W. Yates, in *Proceedings of the International Symposium on In-Beam Nuclear Spectroscopy,* edited by Zs. Dombrádi and T. Fényes (Akadémiai Kiadó, Budapest, 1984), p. 163.
[58]S. W. Yates and G. Molnár, in *Proceedings of the International Research Conference on Nuclear Structure, Reactions, and Symmetries,* edited by R. A. Meyer and V. Paar (World Scientific, Singapore, 1986), p. 632.
[59]G. Wenes, P. Van Isacker, M. Waroquier, K. Heyde, and J. Van Maldegham, Phys. Rev. C **23**, 2291 (1981). Although unnatural parity levels were calculated for bands "2" and "3," they were inadvertently left out of Fig. 1 of this reference. Their excitation energies were kindly provided by K. Heyde.
[60]G. Bonsignori, M. Savoia, K. Allaart, A. Van Egmond, and G. te Velde, Nucl. Phys. **A432**, 389 (1985); G. Bonsignori, K. Allaart, and A. Van Egmond, Prog. Part. Nucl. Phys. **9**, 431 (1983).
[61]D. Janssen, R. V. Jolos, and F. Dönau, Nucl. Phys. **A224**, 93 (1974).
[62]A. Arima and F. Iachello, Ann. Phys. (N.Y.) **99**, 253 (1976).
[63]K. Allaart, G. Bonsignori, M. Savoia, and V. Paar, Nucl. Phys. **A458**, 412 (1986).
[64]K. Allaart, E. Boeker, G. Bonsignori, M. Savoia, and Y. K. Gambhir, Phys. Rep. **169**, 209 (1988).
[65]D. F. Coope, S. N. Tripathi, M. C. Schell, J. L. Weil, and M. T. McEllistrem, Phys. Rev. C **16**, 2223 (1977).
[66]O. Bohigas, M. J. Giannoni, and C. Schmit, Phys. Rev. Lett. **52**, 1 (1984).
[67]T. A. Brody, J. Flores, J. B. French, P. A. Mello, A. Pandey, and S. S. M. Wong, Rev. Mod. Phys. **53**, 385 (1981).
[68]T. H. Seligman, J. J. M. Verbaarschot, and M. R. Zirnbauer, Phys. Rev. Lett. **53**, 215 (1984); J. Phys. A **18**, 2751 (1985).
[69]D. Delande and J. C. Gay, Phys. Rev. Lett. **57**, 2006 (1986); **57**, 2877 (1986).
[70]D. Wintgen and H. Marxer, Phys. Rev. Lett. **60**, 971 (1988).
[71]D. C. Meredith, S. E. Koonin, and M. R. Zirnbauer, Phys. Rev. A **37**, 3499 (1988).
[72]M. V. Berry and M. Tabor, Proc. R. Soc. London Ser. A **356**, 375 (1977).
[73]G. Casati, B. Chirikov, and I. Guarneri, Phys. Rev. Lett. **54**, 1350 (1985).
[74]T. Cheon and T. D. Cohen, Phys. Rev. Lett. **62**, 2769 (1989).
[75]P. M. Endt, P. de Wit, and C. Alderliesten, Nucl. Phys. **A459**, 61 (1986); **A476**, 333 (1988).
[76]J. F. Shriner, Jr., E. G. Bilpuch, P. M. Endt, and G. E. Mitchell, Z. Phys. A **335**, 393 (1990).
[77]E. P. Wigner, Oak Ridge National Laboratory Report ORNL-2309, 1957, p. 59.
[78]T. A. Brody, Lett. Nuovo Cimento **7**, 482 (1973).
[79]M. L. Mehta, *Random Matrices and the Statistical Theory of Energy Levels* (Academic, New York, 1967).